

**Development of a Remote Sensing Network for Time-Sensitive
Detection of Fine Scale Damage to Transportation
Infrastructure**

Final Report

DOT Project: OASRTRS-14-H-UNM

Principal Investigator:
Dr. Christopher Lippitt
University of New Mexico

Program Manager:
Mr. Caesar Singh
Office of the Assistant Secretary for Research and Technology
U.S. Department of Transportation

Disclaimer

The views, opinions, findings, and conclusions reflected in this presentation are the responsibility of the authors only and do not represent the official policy or position of the U.S. Department of Transportation/Office of the Assistant Secretary for Research and Technology, or any state or other entity. USDOT/OST-R does not endorse any third party product or service that may be included in this presentation or associated materials.

Executive Summary

This research project aimed to develop a remote sensing system capable of rapidly identifying fine-scale damage to critical transportation infrastructure following hazard events. Such a system must be pre-planned for rapid deployment, automate processing routines to expedite the delivery of information, fit within existing standard operating procedures to facilitate ready use during a hazard response scenario, and the tools need to be commercially available to state DOTs. To design the system and meet these needs, the project team proposed an airborne remote sensing system based on a network of collection platforms, an automated image co-registration and change detection routine, and implementation of all software tools within BAE Systems' GXP line of geospatial software. All image-processing and interpretation tools developed through the project are now commercially available from BAE Systems Inc.

The team's approach to designing the system is based on the Remote Sensing Communication Model, which dictates that the design of time-sensitive remote sensing systems be based explicitly on the needs and properties of the user. The team thus worked closely with the New Mexico Department of Transportation (NMDOT) during the design of the system, including ongoing consultation, attendance of NMDOT workshops and conferences, and two formal surveys: (1) a first phase assessing what infrastructure is considered most critical, the capacity of NMDOT to ingest and leverage geospatial information, and current procedures for monitoring infrastructure after hazard events; and (2) a survey soliciting feedback and evaluating the potential effectiveness of a prototype remote sensing system. Key findings from this effort include: (1) NMDOT does not currently have the capacity, human or infrastructure, to ingest or exploit geospatial data, (2) trust in results requires review by licensed engineers – automated products without engineer review are not perceived as reliable, and (3) NMDOT's definition of critical infrastructure varies substantially from traditional definitions used by the US Federal Emergency Management Agency (FEMA) and other emergency management organizations.

Based on these findings, the following design parameters were adopted and implemented within the remote sensing system: (1) engineer review is part of the information product process, (2), access to data and information products is achieved through standard and ubiquitously available software tools (i.e., web browsers), (3) any geospatial expertise required can be performed by a third party, either through another agency or private contractor, and (4) a standing network of image collection platforms prepared for rapid deployment is required.

The resulting proposed system, which satisfies these design parameters, includes:

- Automated image co-registration, change enhancement, and change detection without human intervention required.
- Web based tools for review by engineers of raw imagery, change enhanced, and change detection images through a web browser. Engineers can provide image clips with annotations and text to report their findings to a central common operating picture.

- Software tools to access and supplement interpreted results during field inspections.
- A relationship with US Air Force auxiliary Civil Air Patrol, who operate a nationally distributed network of aircraft and have as part of their existing mission hazard response and other rapid deployment missions.

Figure A provides a graphic overview of the process. All tools are available commercially within the GXP software platform.

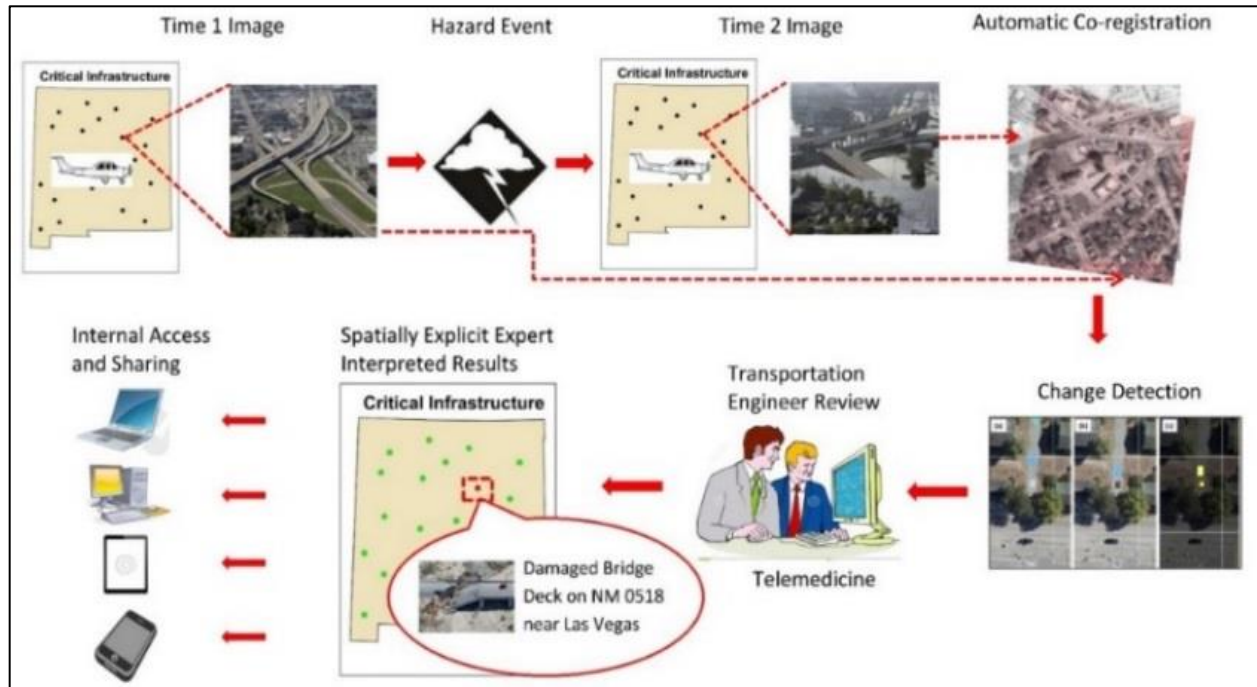


Figure A: Overview of remote sensing system process developed for this project.

Results from the stage 2 “feedback” survey of NMDOT engineers indicate that the system is useful for the inspection of roads and bridges. However, because the system has limited utility for inspecting the superstructure of bridges, confidence is higher when used for inspecting road sections. From the moment the decision is made to deploy the system, it is estimated that information delivery to engineers for remote inspection occurs within 6 hours. This performance rate is currently constrained primarily by the number of platforms available and likely to be improved through introduction of unmanned airborne systems (UAS).

A project website describing the project overview, some example imagery, a video of the Demonstration to FEMA and the DOT, and references to the project in the news and in other scholarly publications, is hosted within the University of New Mexico GIScience for Environmental Management (GEM Lab) webpage: <http://gem.unm.edu/index.php/funded-projects/10-remote-sensing-of-transportation-infrastructure>.

Acknowledgments

The authors wish to thank the United States Department of Transportation (USDOT) Office of the Assistant Secretary for Research & Technology (OST-R) Commercial Remote Sensing and Spatial Information Technologies Program (CRS&SI) for funding this research. We also want to acknowledge the efforts and cooperation of the United States Civil Air Patrol (CAP) for supporting flight activities and working with the project team to assess the feasibility of deploying the system through CAP. The team also owes a debt of gratitude to the members of the Technical Advisory Committee (TAC) and the New Mexico Department of Transportation for working with the project team to ensure the operational feasibility of the developed technologies. TAC members include: Dr. Bruce A. Davis, Lt. Col. John W. Desmarais, Roger Ebner, Stephen Rae, and Timothy Parker, PE.

Glossary

ADAPTEE	Aerial Data Acquisition Processing Transmission-Timeliness Estimator
CAP	Civil Air Patrol
DOT	Department of Transportation
GNSS	Global Navigation Satellite System
GPS	Global Positioning System
NMDOT	New Mexico Department of Transportation
PIO	Public Information Officer
RSCM	Remote Sensing Communication Model
RSI	Repeat Station Imaging
RSS	Remote Sensing Systems
SDSU	San Diego State University
sUAS	Small Unmanned Airborne Systems
TAC	Technical Advisory Council
Tacq	Acquisition Capacity
Tchan	Transmission Capacity
Tdat	Time to Data Delivery
TSRSS	Time Sensitive Remote Sensing System
Trec	Receiver Capacity
UAS	Unmanned Airborne Systems
UNM	University of New Mexico

Table of Contents

Disclaimer	1
Executive Summary.....	2
Acknowledgments	4
Glossary	5
List of Figures	7
List of Tables	8
Chapter 1: Introduction	9
Chapter 2: Initial Survey of New Mexico DOT.....	11
Chapter 3: System Architecture.....	13
Chapter 4: Optimization of Image Acquisition.....	15
ADAPTEE	15
Total Time to Information Delivery	16
Analytical model for Repeat Station Imaging.....	19
Chapter 5: Algorithm Development.....	21
Automated image co-registration	21
Automated change detection	24
Shadow correction	30
Chapter 6: Software Implementation.....	34
Chapter 7: Post-prototype Survey.....	40
Chapter 8: Commercialization Plan	42
Chapter 9: Conclusions	45
References.....	46
Appendices	49
Appendix A: Summary of Tasks.....	49
Appendix B: TAC Meeting Minutes.....	49
Appendix C: Media, Publications, and Presentations	49

List of Figures

Figure A: Overview of remote sensing system process developed for this project.....	3
Figure 3.1: Overview of remote sensing system process developed for this project.....	13
Figure 3.2: The software architecture and process utilized in this project.....	14
Figure 4.1: Chart of modeled vs. measured differential parallax, for image frame pairs captured with a range of horizontal imaging station offsets at two altitudes.....	20
Figure 5.1: Result of feature-based image matching.....	22
Figure 5.2. RMSE values for 222 image pairs co-registered using the 7 Mar2016 software version.....	23
Figure 5.3. RMSE values for 148 image pairs co-registered using the 3 Apr 2016 software version.....	24
Figure 5.4. Difference images for a bridge in Albuquerque, NM.....	26
Figure 5.5. Time-1, time-2, and change images (black = no change, white = change) for an area on Camp Roberts, CA, with abandoned barracks and a marching deck.....	27
Figure 5.6. Zoomed in view of final change product.....	29
Figure 5.7. Bi-temporal shadow classification maps of the four study scenes, corresponding to (a) frames <i>a</i> and <i>b</i> (hospital facility), (b) <i>c</i> and <i>d</i> (office park), (c) <i>d</i> and <i>e</i> (university campus), and (d) <i>f</i> and <i>g</i> (bridge overpass).....	31
Figure 5.8. Comparison of intensity image difference products based on the normalized images versus the original intensity images.....	32
Figure 5.9. Magnified subsets of the intensity and arithmetical difference products, based on normalized images <i>versus</i> original images.....	32
Figure 6.1: Overview figure showing how the software tools relate to the project workflow.....	34
Figure 6.2. SOCET GXP showing time-2 image (top left), time-1 image (bottom left), multicolored change enhancement image (top right) and change detection result (bottom right) showing changes between the time-1 and time-2 images.....	36
Figure 6.3. Finding images for an Image Station in GXP Xplorer.....	37
Figure 6.4. GXP WebView with multiple image layers.....	38
Figure 6.5: Selecting an image in GXP Xplorer Mobile.....	39

List of Tables

Table 4.1. Model fit for acquisition time.....	16
Table 4.2. Model fit for transmission time.....	16
Table 4.3. Receiver Capacity sub model fit.....	17
Table 4.4. Total time to information delivery estimates for 6 cm GSD collections.....	18
Table 4.5. Total time to information delivery estimates for 12 cm GSD collections.....	18
Table 5.1. Co-registration accuracy and reliability measures for a range of image sets tested....	23

Chapter 1: Introduction

Immediately following a hazard event (e.g., earthquake, flood, tsunami, wildfire passage, nuclear accident, etc.), transportation and emergency managers need validated situational awareness of the status of critical transportation infrastructure (e.g., roads, bridges, railways, airports, etc.). The most reliable, detailed, and comprehensive means for early and documentable reconnaissance of post-event damage assessment is through low cost airborne imaging systems supported by semi-automated image processing and analysis, and coordinated image/map dissemination capabilities.

As the only synoptic sensing technology available, remote sensing represents a critical source of information on the status of transportation infrastructure following hazard events. The timescales in which information on infrastructure status is required following hazard events, however, presents challenges to the traditionally *ad hoc* network of platforms, sensors, and analysts employed by remote sensing. While satellite imagery is a common source of information following natural disasters, its utility for transportation infrastructure monitoring is limited by the spatial and temporal resolution of current and planned space-borne systems (0.5 m spatial resolution at the finest, and imaging opportunities once per day for a limited number of high spatial resolution satellite sensors). Therefore, the need for actionable intelligence to support responses to natural hazard events provides an impetus to move airborne remote sensing into a role of rapid data collection and dissemination. Technological advances enable airborne image acquisition, processing, and dissemination in times sufficient to satisfy information requirements of time sensitive decision-making (Stryker and Jones 2009). However, the complexity of tasking, data collection, processing and transfer, and information distribution from the range of available airborne remote sensing systems presents a critical challenge to the effective use of remote sensing to support hazard response.

This project aimed to develop a remote sensing system capable of rapidly identifying fine-scale damage to critical transportation infrastructure following hazard events. Such a system must be pre-planned for rapid deployment, automate processing routines to expedite the delivery of information, fit within existing standard operating procedures to facilitate ready use during a hazard response scenario, and the tools or information need to be readily available to DOTs. To design the system and meet these needs, the project team designed an airborne remote sensing system based on a network of collection platforms, an automated image co-registration and change detection routine, and implementation of all software tools within BAE Systems' GXP line of geospatial software.

The New Mexico Department of Transportation (NMDOT) served as a prototypical state DOT for whom the system was designed. A series of interviews and other less formal interactions with NMDOT engineers and other transportation and hazard response professionals were used to inform each stage of the design of the system. Implementation of the system necessitated a series of research development tasks related to optimization of acquisition strategy, automation of processing routines, detecting changes potentially related

to infrastructure damage, and optimizing the information production and distribution workflow to generate and deliver information to infrastructure and emergency managers. What follows is a description of those research and development activities.

Chapter 2: Initial Survey of New Mexico DOT

The design of the system was based on the Remote Sensing Communication Model (RSCM), which dictates that the design of time-sensitive remote sensing systems be based explicitly on the needs and properties of the user (Lippitt et al. 2014). Because of the compressed decision timescales of hazard response scenarios, successful use of the TSRSS-based approach requires a pre-designed system ready to deploy and deliver reliable information. Therefore, a two-stage survey process was adopted to ensure the designed system could integrate with NMDOT's existing operating procedures.

The initial survey was designed to determine which types of transportation infrastructure and damage are considered truly critical and the standard operating procedures and capacity of the user, which in this case is NMDOT. The stage 1 survey used open-ended questions to determine current transportation infrastructure damage assessment procedures and decision processes. Questions were structured to determine current technical capacity, experience, and resources. In the stage 2 survey, transportation managers were provided with damage change detection products produced by the prototype system and asked to assess product utility and desirability in the context of their anticipated decision requirements under various hazard scenarios in their jurisdiction. Surveys were conducted by videoconference and phone to maximize participation and minimize travel costs.

A total of 26 interviewees were identified from NMDOT for the stage 1 survey. These interviewees are from various NMDOT districts (six districts in total), bureaus, offices, and divisions. Survey responses were obtained from 13 of them (50% response rate). Different districts or divisions manage different transportation infrastructure assets, indicating that it is necessary to coordinate among various divisions during a hazard event that involves various transportation infrastructure assets. Critical transportation infrastructure is not readily defined or tracked in NMDOT's general office or district offices. According to the interviewees, any type of transportation infrastructure could be critical depending on the hazard event situation and/or location. Bridges are typically considered the most critical transportation infrastructure assets, followed by roadways. The factors that cause a bridge or roadway to be critical are the traffic volume that it provides services to and its location, though interviewees were not generally aware of how critical transportation infrastructure is to evacuation, resource routing, or other disaster response activities. Damage evaluation metrics for bridges and roadways were also obtained from NMDOT.

Currently, NMDOT does not use any remote sensing techniques for post-disaster infrastructure inspection and hazard response purposes. The primary inspection method that they use is "boots on the ground"; patrol engineers visually inspect the transportation infrastructure assets in person. Throughout the event, patrol crews consisting of several transportation engineers will actively monitor the transportation infrastructure assets involved in hazard events 24 hours a day until the hazard event has ceased. The patrol crews will report

the disaster situation to the district engineer and assistant district engineer for maintenance and they will work with State Maintenance Bureau for further decisions. The State Maintenance Bureau will also provide support to the affected district if needed. However, these patrol crews do not have the authority to restrict access to these assets, and only the New Mexico State Police have the authority to enforce access. The general office and district offices have Public Information Officers (PIOs) who are responsible for information released to the public. However, transportation infrastructure damage information is released to the public only by request or indirectly through the state police or Emergency Operations Center, although multiple methods (e.g., radio, TV, email, website) are available to provide the information to the public.

Key takeaways from the stage 1 survey directly informed the design of the system. These include that fact that NMDOT does not have the internal capacity to implement such a system and that inspection by trained and licensed engineers is the current standard.

Chapter 3: System Architecture

To permit rapid inspection of infrastructure features, the system was designed based on a change detection approach to permit identification of changes introduced by a hazard event, as opposed to only a post-hazard survey that would require detailed inspection of the infrastructure. To permit rapid and precise registration of baseline image sets to post-hazard image sets, a repeat station imaging (RSI) approach was adopted (Coulter et al 2003). Because current NMDOT procedures currently rely on inspection by certified engineers, the system was designed to include crowd-sourced inspection by vetted engineers and only their interpretations put into a central common operating picture accessible to emergency managers. Out of a desire to make the developed system accessible to Departments of Transportation by the termination of the project, all tools were developed within the SOCET GXP line of geospatial software produced, sold, and supported by BAE Systems Inc.

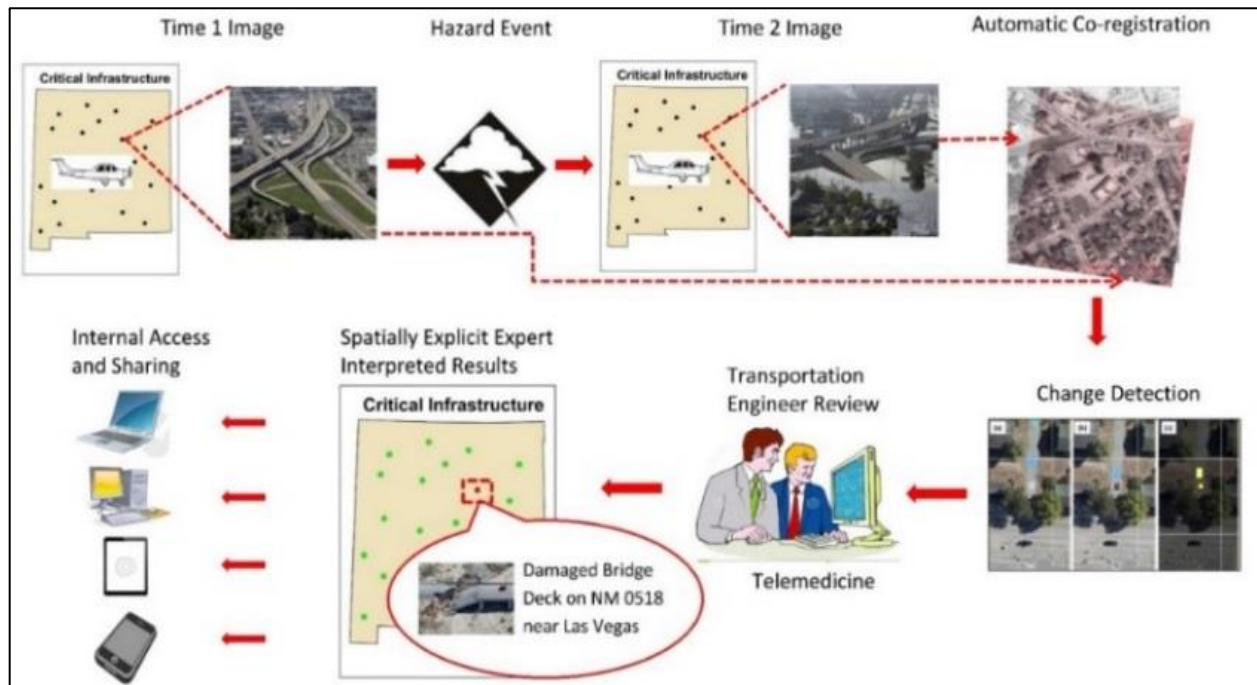


Figure 3.1: Overview of remote sensing system process developed for this project.

SOCET GXP is BAE Systems' well known desktop software application for image analysis, geospatial analysis, photogrammetry and mapping (BAE Systems, 2017). As part of this project, BAE Systems customized and enhanced existing capabilities to perform frame-based co-alignment of RSI airborne image pairs, perform change detection and enhancement, and permit remote interpretation of those changes by engineers. The overall software workflow is shown in Figure 3.1 and a more complete description of the software architecture can be found Figure 3.2. The system employs several discrete software packages offered by BAE Systems, including: (1) the desktop application SOCET GXP for bulk processing by a single trained analyst, (2) GXP

WebView for remote inspection by engineers, (3) GXP Explorer for cataloguing, and (4) GXP OnScene for accessing and supplementing results based on field inspections.

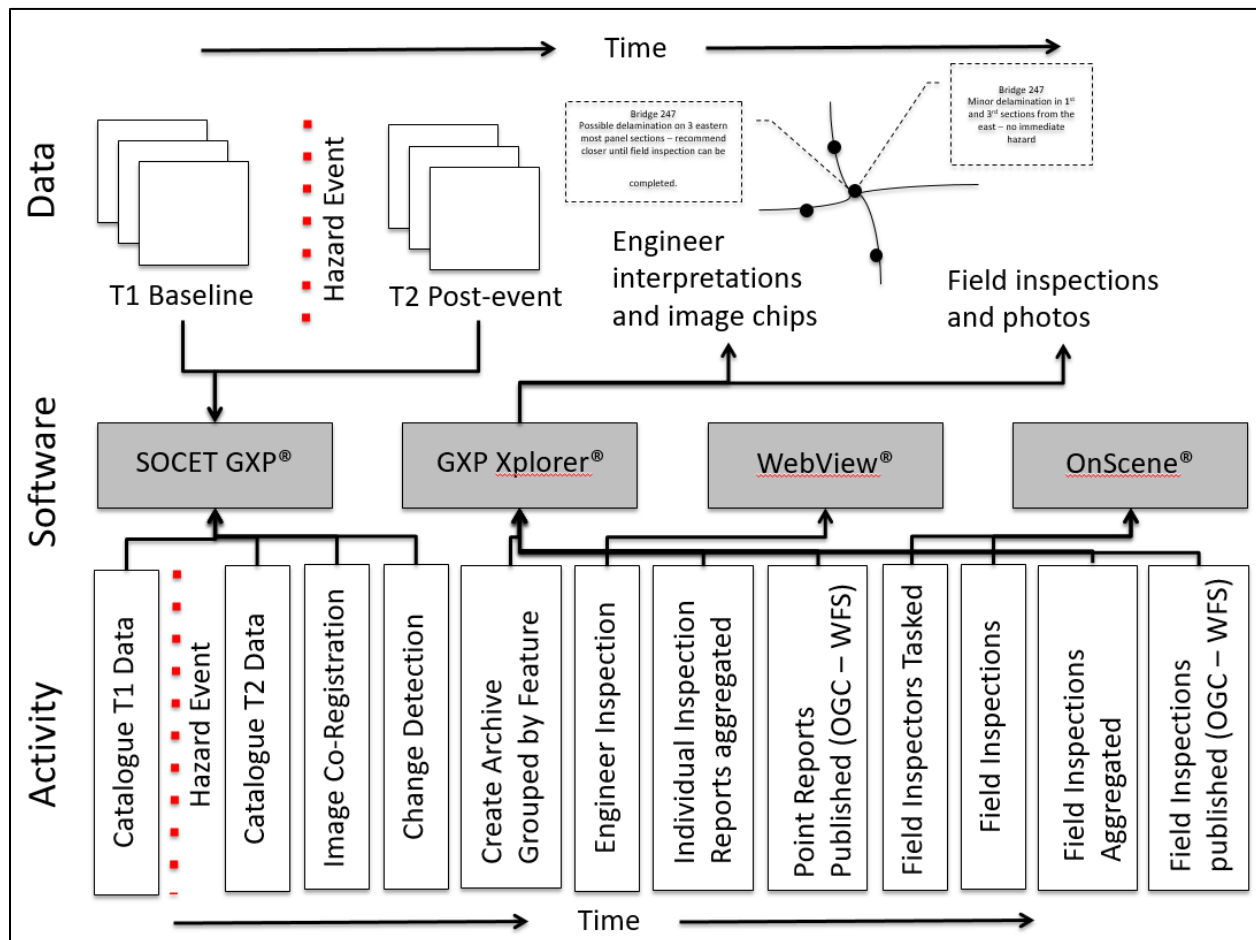


Figure 3.2: The software architecture and process utilized in this project.

The following sections describe the major research development tasks required to optimize image collection, automate and optimize image co-registration, optimize change detection, and implement all developments within the SOCET GXP platform.

Chapter 4: Optimization of Image Acquisition

ADAPTEE

Timeliness is defined as “the time between information request and the use of that information to inform a decision.” Predicting the timeliness of time-sensitive remote sensing systems prior to operational deployment is a requirement. When compared to satellites, aircraft acquisitions have additional factors affecting timeliness that make it challenging to incorporate them into the standard operating procedures of emergency management organizations. The number of aircraft, their locations relative to areas at high risk for disasters, the types of aircraft, and the imaging sensors they operate, all affect the timeliness of data acquisition and delivery.

The Remote Sensing Communication Model (RSCM) was created, in part, to provide a means for assessing the timeliness of information delivery under various remote sensing systems (RSS) configurations. RSCM capacity analysis was automated through the development of the Aerial Data Acquisition Processing Transmission – Timeliness Estimator (ADAPTTE) to make estimation of acquisition and transmission timeliness in the RSS design phase routine, but also enables on-the-fly estimation of time to data delivery (TDat) to aid in asset tasking (i.e., dynamic RSS configuration) during the response phase of the hazard cycle.

The RSCM conceptualizes RSS as having capabilities that determines the timeliness of discrete segments (i.e., sensors, channels, and receivers), each with a capacity that determines the timeliness of that segment based on the data volume to be acquired: acquisition capacity, transmission capacity, and receiver capacity (i.e., a human/machine analyst to produce information). ADAPTTE’s ability to model the timeliness of data delivery to analyst (i.e., sensor and channel capacity) was validated by comparison of estimates to a series of actual flight data records, which record time and location of the aircraft through GPS records.

Accuracy assessment using eight manned and four unmanned flights was conducted to empirically test the predictions from ADAPTTE. Table 4.1 shows the model fit for acquisition time and Table 4.2 shows the model fit for transmission time. The results clearly indicate improved model fit when human pilots are not directly operating the aircraft platform but also suggest that integration of additional information affecting TDat (e.g., pilot’s assessment of planned flight path, airspace information, and ground elevation data) would reduce the overall error.

Table 4.1. Model fit for acquisition time

Variable	Manned Only (R^2_{adj})	Manned Only RMSE	Manned & UAS (R^2_{adj})	UAS Only RMSE
T_{Acq}	0.310	3612	0.751	2
B_S/C_{Acq}	0.953	249	0.985	2
T_M	0.686	364	0.937	1
T_D	0.053	3560	0.409	1

Table 4.2. Model fit for transmission time.

Variable	(R^2_{adj})	RMSE
T_{Chann} : Modeled Volume	0.997	77
T_{Chann} : Actual Volume	0.987	199
B_S : Data Volume	0.986	----

According to ADAPTTE models run for six example critical infrastructure imaging missions, the introduction of sUAS has the potential to reduce the time required for data acquisition in situations where the critical infrastructure spans an area small enough that the number of simultaneous sUAS operating in a ‘swarm’ is neither cost-prohibitive nor technically impossible. The sUAS are also more accurately modeled for their timeliness capacities than manned aircraft.

Results clearly demonstrated that the RSCM can be used for modeling the acquisition and transmission timeliness of dynamically configurable RSS. For more information about data timeliness, please refer to the report of “Report Detailing Total Time to Information Delivery under Various TSRSS Configurations”.

Total Time to Information Delivery

The Remote Sensing Communication Model (RSCM) permits the estimation of the timeliness of remote sensing systems (RSS). As mentioned above, the RSCM conceptualizes RSS as having capabilities that determines the timeliness of discrete segments (i.e., sensors, channels, and receivers), each with a capacity that determines the timeliness of that segment based on the data volume to be acquired: acquisition capacity, transmission capacity, and receiver capacity (i.e., a human/machine analyst to produce information). This section focuses on summarizing the validation of the receiver capacity and total time to information delivery under various TSRSS configurations. The timeliness for the receiver capacity was benchmarked using the automated procedures developed through the project and implemented in BAE Systems SOCET GXP software package. SOCET GXP 4.2.0 was installed on a server-based virtual machine (VM) to allow manipulation of machine specifications required for software performance benchmarking (i.e., receiver capacity).

The specification of the physical server is 12 cores (1.9 Ghz per core) from 2 Intel Xeon ES-2420, 6 core CPUs. The VM installed on this server was configured with Windows 10 and 32 GB of RAM. The number of cores assigned to the virtual machine and the number of image pairs (dataset size) used within SOCET GXP were manipulated to assess their impact of performance. Each combination was tested three times and averaged to estimate receiver capacity. It is a best practice to run each test multiple times (normally three times) and calculate the average result because fluctuations in background processes on a machine can cause inaccurate time results. In addition, any anomalous results were excluded. The timeliness of receiver capacity was assessed from one pair to 32 image pairs and using 2 to 8 cores in 2 core increments.

Based on benchmarking results, the operations were modeled as three discrete functions: frame import, batch processing, and human time. The models developed for frame import and human time work effectively with a higher certainty ($R^2 > 0.95$) and lower errors (mean percent error $< 26\%$) when compared with batch processing. It should be noted that the model for the batch processing still works effectively, but with a medium certainty ($R^2 = 0.73$) and higher errors ($\sim 40\%$ mean percent error). It is possible that there are outliers in the batch processing performance, which additional benchmarking tests could address. Table 4.3 shows the model fit for receiver capacity models.

Table 4.3. Receiver Capacity sub model fit.

Model ID	Mode Description	R^2	Mean Percent Error
1	Frame Import	0.96	18.02%
2	Batch Processing	0.73	39.95%
3	Human Time	0.97	25.61%

With the receiver capacity calculated, it is possible to report the total time to delivery of information under various TSRSS configurations when combined with models of acquisition capacity and transmission capacity. Table 4.4 reports the total time for the 6 cm ground sampling distance (GSD) datasets in New Mexico and Table 4.5 reports the total time for 12 cm GSD datasets in New Mexico. In these tables, Tdat indicates the total time, Tacq indicates acquisition capacity, Tchan indicates transmission capacity, and Trec indicates receiver capacity.

Table 4.4. Total time to information delivery estimates for 6 cm GSD collections.

Platform	Sensor	Bit Depth	Bands	South Capital Complex				Cochiti Lake				Sandoval Detention Center			
				Tdat (h)	Tacq (h)	Tchan (h)	Trec (h)	Tdat (h)	Tacq (h)	Tchan (h)	Trec (h)	Tdat (h)	Tacq (h)	Tchan (h)	Trec (h)
Cessna TU206G	Ultracam X - 100mm	12	4	8.20	6.03	2.00	0.16	8.88	6.57	2.05	0.25	7.65	5.53	2.00	0.12
	Ultracam X - 100mm	8	3	8.19	6.03	2.00	0.15	8.80	6.57	2.05	0.20	7.62	5.53	2.00	0.09
Cessna 182	Canon 6D - 100mm	14	3	1.59	1.38	0.03	0.16	4.79	3.30	1.27	0.24	0.89	0.77	0.01	0.11
	Canon 6D - 100mm	8	3	1.56	1.38	0.02	0.15	4.20	3.30	0.70	0.20	0.86	0.77	0.01	0.09
Piper Navajo	DMC 1 - 120mm	12	4	8.85	6.70	2.00	0.16	9.97	7.65	2.05	0.25	9.11	6.98	2.00	0.12
	DMC 1 - 120mm	8	3	8.86	6.70	2.00	0.15	9.89	7.65	2.03	0.20	9.08	6.98	2.00	0.09

Table 4.5. Total time to information delivery estimates for 12 cm GSD collections.

Platform	Sensor	Bit Depth	Bands	South Capital Complex				Cochiti Lake				Sandoval Detention Center			
				Tdat (h)	Tacq (h)	Tchan (h)	Trec (h)	Tdat (h)	Tacq (h)	Tchan (h)	Trec (h)	Tdat (h)	Tacq (h)	Tchan (h)	Trec (h)
Cessna TU206G	Ultracam X - 100mm	12	4	8.14	6.00	2.00	0.14	8.30	6.12	2.00	0.18	7.57	5.52	2.00	0.06
	Ultracam X - 100mm	8	3	8.11	6.00	2.00	0.11	8.29	6.12	2.02	0.17	7.55	5.52	2.00	0.04
Cessna 182	Canon 6D - 100mm	14	3	1.44	1.30	0.02	0.13	2.61	2.12	0.32	0.17	0.79	0.73	0.01	0.05
	Canon 6D - 100mm	8	3	1.42	1.30	0.01	0.11	2.47	2.12	0.18	0.17	0.78	0.73	0.01	0.04
Piper Navajo	DMC 1 - 120mm	12	4	8.80	6.67	2.00	0.14	9.38	7.18	2.00	0.18	9.03	6.97	2.00	0.06
	DMC 1 - 120mm	8	3	8.77	6.67	2.00	0.11	9.37	7.18	2.02	0.17	9.01	6.97	2.00	0.04

Total time to information delivery is projected to be between 0.78-9.97 hours after initial request for information for the example targets. Note that these example targets represent larger collections that would be expected in real hazard scenario and therefore represent conservative estimates of delivery time. In practice, ADAPTTE can be used to design flight plans and estimate information delivery time on the fly, allowing managers to dynamically adjust the scope of the mission based information delivery time requirements. For more information about total time to information delivery, please refer to the report “Total Time of Information Delivery of the Optimized TSRSS”.

Analytical model for Repeat Station Imaging

Achieving precise spatial co-registration of high spatial resolution multitemporal imagery in near real-time using automated procedures is not trivial and is dependent on employing a Repeat Station Imaging (RSI) collection strategy (Coulter *et al.* 2003; Stow *et al.* 2003; Coulter and Stow 2005; Coulter and Stow 2008; Coulter *et al.* 2012). The RSI method is based upon matching imaging stations in terms of horizontal position and altitude between multitemporal image acquisitions. When image frames are captured from exactly the same imaging station in the sky over time, there is no parallax between images and they exhibit the same terrain-related geometric distortions (they are essentially carbon copies of each other). Therefore, precise co-registration may be achieved when images from matched imaging stations are co-registered on a pairwise basis using a simple, automated geometric transformation model. Matching image stations repeatedly over time is most effectively accomplished through the use of global navigation satellite systems (GNSS) (such as GPS) to aid the pilot/aircraft in maintaining the desired track and altitude, and automatically trigger image capture at predetermined imaging stations (Coulter *et al.* 2003).

Some level of error in camera station matching is inevitable. This may be due to inherent errors in the GNSS/GPS system used, pilot or autopilot delays in course correction, high winds, etc. The accuracy of image co-registration between RSI image frames (i.e., images captured from the same camera stations over time) depends upon several factors including: (1) aircraft/sensor altitude, (2) height of three-dimensional (3D) features within the image scenes such as buildings or terrain relief, and (3) the horizontal and vertical accuracy with which image stations are matched when collecting multitemporal image sets. To elucidate how these factors interact to affect co-registration accuracy, an analytical model was developed based on established photogrammetric principles. The same model may be inverted to dictate image collection parameters required to achieve a specified level of image co-registration for specific locations and/or applications.

When each type of offset (horizontal and vertical) or difference in sensor orientation is considered separately, the team found that relative displacement of features in RSI pairs are linear functions of the varying orientation parameters and focal length, except for an inverse square relationship with height above ground level. To validate the analytical model, airborne imagery with 0.08 m (3-inch) spatial resolution was collected over San Diego State University. Using an 11-story tall residential tower, differential parallax was calculated using one of the analytical model equations (one that considers only horizontal offset in camera stations over time) and compared that measurement to the measured differential parallax within the custom airborne imagery collected. This was performed for two sets of four images captured at different altitudes with 50 mm and 105 mm lenses (both sets achieving 0.08 m spatial resolution). The team demonstrated that the analytical model equation accurately predicted the measured differential parallax (Figure 4.1). In addition to showing strong agreement between modeled vs. measured values, the chart in Figure 4.1 also shows that differential parallax values for image frames captured at 5400 ft above ground level (AGL) with the 105 mm

lens are approximately half of corresponding differential parallax values for image frames captured at 2700 ft AGL with the 50 mm lens. This finding supports relationships described by the analytical model and suggests that a high altitude, long focal length acquisition strategy is most appropriate for the automated change detection approach. Further information may be found in the submitted report “Evaluation of Geometric Capture and Processing Elements in the Context of a Repeat Station Imaging Approach to Registration and Change Detection” or in the peer-reviewed publication that resulted from this work (Stow et al., 2016a).

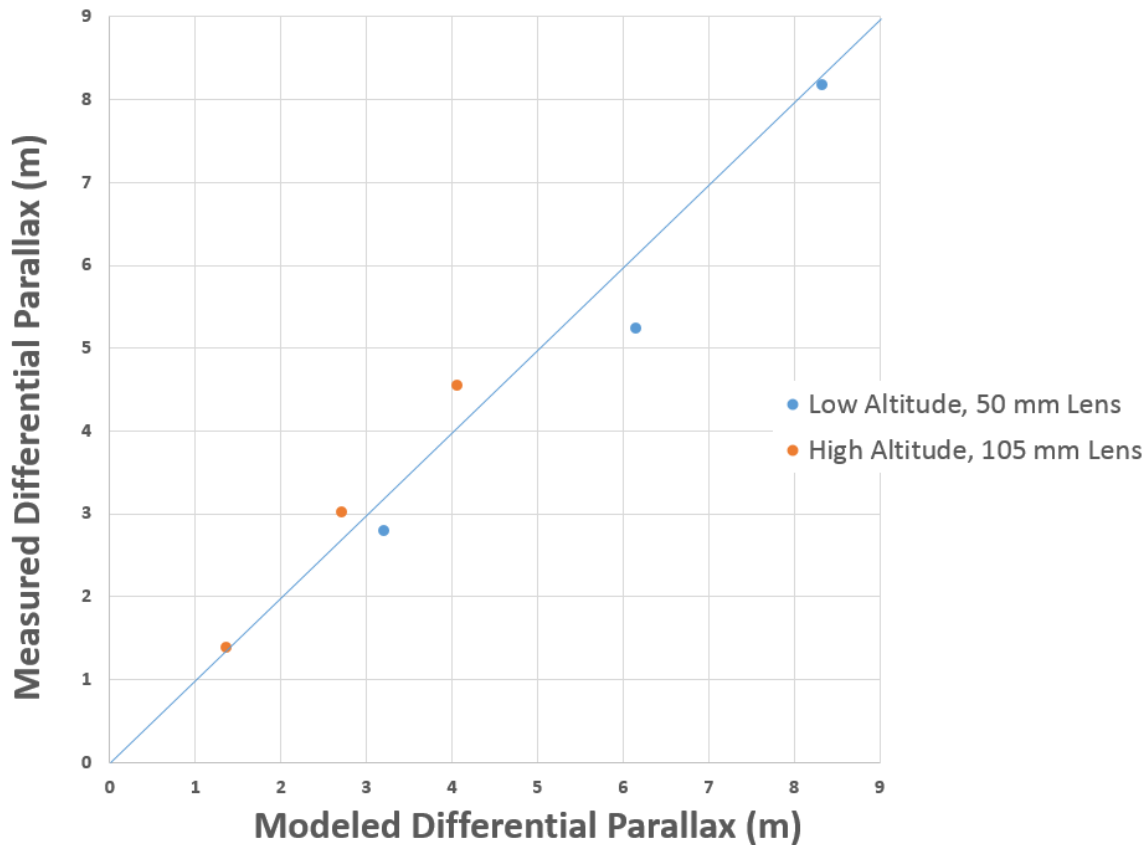


Figure 4.1. Chart of modeled vs. measured differential parallax, for image frame pairs captured with a range of horizontal imaging station offsets at two altitudes.

Chapter 5: Algorithm Development

Change detection is dependent on image co-registration quality (Toutin 2004), radiometric alignment between image pairs (Song et al. 2001), and the change detection algorithm applied (Chan et al. 2001). These three areas were therefore the focus of the team's algorithm development efforts.

Automated image co-registration

As a result of the RSI process, the time-1 and time-2 images are usually rather similar and it is usually a straightforward process automatically to find corresponding points in the two images, then estimate the parameters of a two-dimensional transformation that can be applied to the time-1 image to bring it into the same coordinate space as the time-2. In the early phase of the development, the main focus was on the image matching, in order to measure well distributed, accurate tie points between time-1 and time-2 images. Different approaches have been developed and tested. A hybrid approach using a combination of OpenCV feature-based (Bradski and Kaehler 2008; Rublee *et al.* 2011) and BAE Systems' area-based tie point matchers was selected and implemented in the SOCET GXP® desktop processing software.

The feature-based tie point matcher combined with RANSAC (Random Sample Consensus) can find tie points even when there is a large shift and/or rotation between the two images of the pair, though the use of RSI usually ensures that the situation is much better than this, for example the change in scale between the images is typically quite small. In Figure 5.1, the white lines connect the tie points matched between the time-1 and time-2 images. The tie points are all on obvious features, so there is no guarantee of a good geometric distribution in the overlap area. The accuracy of this feature-based matching is not at the sub-pixel level, which could be achieved by the area-based tie point matcher. On the other hand, the area-based tie point matcher can produce an incorrect match when the images have a large initial relative georeferencing error.



Figure 5.1: Result of feature-based image matching. Typically, the lines joining matches points are approximately parallel – this enables easy visualization of bad matches such as the one between moving cars near the bottom of the images.

The tie points derived from the approach above are used to compute the transformation between the image pair. Affine and 2D polynomial algorithms are used in this stage. A new registered time-1 image is created based on the time-1 to time-2 image transformation. The newly created, registered time-1 image is in the same image and ground space as the time-2 image.

Over 300 image pair combinations were utilized for automated image co-registration testing. These included images from multiple camera stations along individual flight lines at each site, and multiple combinations of repeat-pass image sets (either from the same time of day, or return visits hours or weeks later) from each camera station. Results indicating the accuracy and reliability of the RSI-ACD automated image co-registration software are provided in Table 5.1 and Figures 5.2 and 5.3. Table 5.1 provides results for AM/AM (same time of day) and AM/PM (different time of day, same day or two weeks apart) image pair co-registration. For the AM/AM pairs with similar shadow conditions, 92%-95% of image pairs co-registered with a root mean square error (RMSE) less than 2 pixels, and 98%-96% of image pairs co-registered with a RMSE less than 4 pixels. Only a small percentage of image pairs (2%-4%) co-registered with RMSE values greater than 4 pixels. In addition, 2%-3% of input images failed co-registration and were not output.

Table 5.1. Co-registration accuracy and reliability measures for a range of image sets tested. The RMSE range percentages were computed based upon the number of image pairs that were output from the software and sum to 100%. The “% Failed” percentages were calculated separately, based upon the number of total images input into the software (these counts are not shown).

Time of Day & Version (3/7 or 4/3)	# Image Pairs Output by Software	% RMSE <= 2.0 Pixels	% RMSE Between 2-4 Pixels	% RMSE > 4.0 Pixels	% Failed
AM/AM – 3/7 version	156	95%	3%	2%	3%
AM/AM – 4/3 version	61	94%	3%	3%	2%
AM/PM – 3/7 version	66	20%	4%	76%	31%
AM/PM – 4/3 version	87	44%	18%	38%	14%

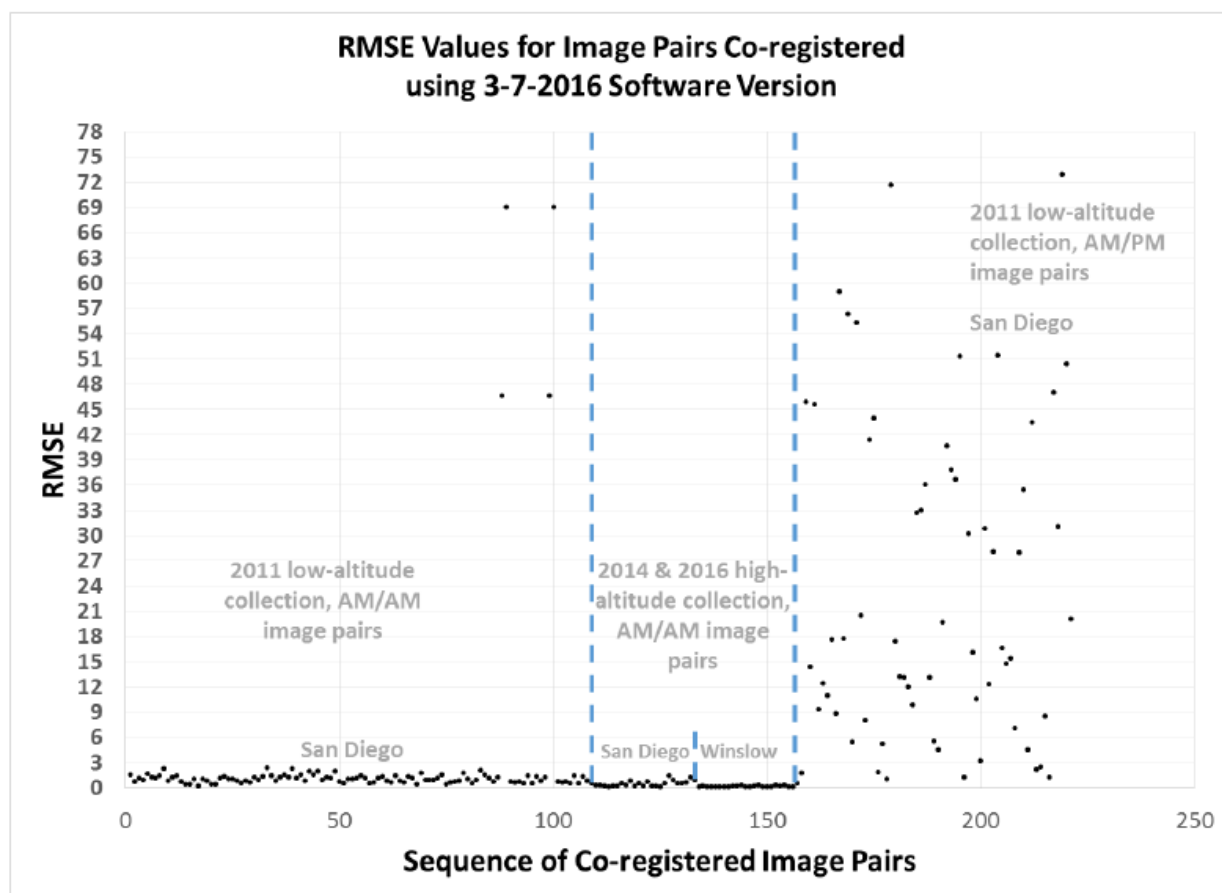


Figure 5.2. RMSE values for 222 image pairs co-registered using the 7 Mar2016 software version. Effects of image collection and scene parameters on co-registration accuracy are apparent.

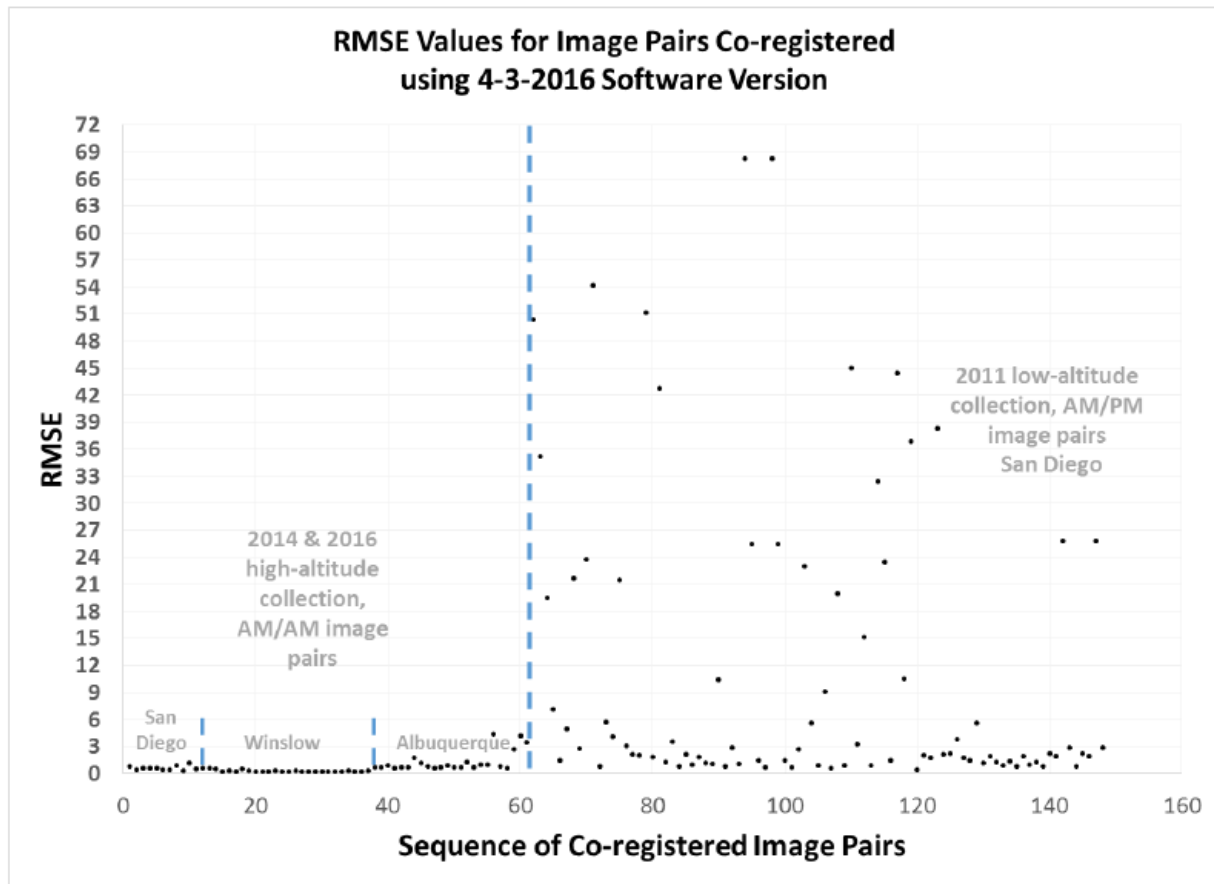


Figure 5.3. RMSE values for 148 image pairs co-registered using the 3 Apr 2016 software version. Effects of image collection and scene parameters on co-registration accuracy are apparent.

Several findings stem from the interpretation of Figures 5.2 and 5.3. Firstly, 2011 low-altitude AGL AM/AM images generally have registration errors of under 3 pixels (RMSE). Secondly, 2014 and 2016 high-altitude AGL AM/AM image pairs achieve consistently higher registration accuracy (approximately 1-1.5 pixels). This result is consistent with the findings of Stow *et al.* (2016), as flying at higher altitudes AGL reduces differential parallax between images (assuming consistent camera station matching errors) and yields improved co-registration when using the RSI technique. The AM/AM image pair results for the Winslow site yielded the highest co-registration accuracy values (averaging 0.3 pixel RMSE). This result is attributed to (1) high altitude collection, (2) relatively low terrain relief within the imaged scenes, and (3) precise flying that replicated camera stations closely.

Automated change detection

In order to simultaneously meet the information needs and timeliness standards required for rapid situational awareness and safety of first responders in the field, an automatic, rapid and robust method of detecting meaningful changes in transportation infrastructure is needed. The product created by such a process is designed for assisting an image analyst in

identifying road and bridge surfaces or sub-structures that have been damaged by highlighting changes of interest and suppressing changes not of interest. The final output should present a before and an after image with those detected change features that have a direct influence on road and bridge safety. To this end, an automated change detection workflow designed specifically to detect cracks in road and bridge surfaces using before and after images captured with digital frame cameras in the visible portion of the spectrum was developed.

There are several challenges associated with the creation of an automatic change detection workflow designed to specifically delineate small (8 – 16 cm width) cracks in road and bridge surfaces. First, minor misregistration of the image pairs causes offset areas to be falsely detected as change. The use of the RSI approach during image capture and processing helps to greatly reduce misregistration and associated false detections, but does nothing to eliminate the detection of real changes not associated with road surface damage (i.e., not of interest). Another challenge is that the targets to be detected (cracks) are small and lack a distinctive spectral signature that could be used in their detection. The most common changes detected that are not of interest include the movement of cars and people over the road surface, changes in shadow position, and seasonal changes in the phenology of overhanging vegetation. To detect and delineate cracks while simultaneously eliminating the detection of changes not of interest, several image enhancement and spatial filtering techniques were employed.

To develop a successful method of detecting and delineating cracks in road and bridge surfaces, the specific form in which a crack manifests in a bi-temporal image pair must be understood and leveraged. The creation of visually simple products displaying only relevant changes is critical. As can be seen in Figure 5.4, a difference image containing all brightness changes could be very difficult to interpret, and would provide little or no benefit over simply viewing the before and after image side by side. In Figure 5.4, the values of the difference image indicate brightness difference over time, and many of the high magnitude difference values associated with shadow position change could result in false detection of changes of interest.

Within high spatial resolution aerial images, a new crack on a bridge/road surface will appear as an elongated, linear area that is darker than its pavement background, and from time-1 to time-2 the area of the new crack will exhibit a decrease in brightness. To this end, the developed detection model is only sensitive to negative changes in brightness and will disregard any detection that do not fit the linear spatial profile of a crack.

In order to compensate for small misregistration effects, a kernel based focal minimum filter is applied to the time-1 image. This filtering technique minimizes the effects of slight misregistration by comparing the DN values in the time-2 image to the minimum value of DNs contained in the kernel window of time-1. This has the effect of forcing the value of the time-2 pixel to be less than the minimum value contained in that focal window to be considered a true change. For example, in a case where a narrow feature such as a crack is misregistered by two pixels, the change detection routine would display the misregistered position in time-2 image as a change, when in fact there is only one feature that is misregistered and has not changed. The focal minimum filter effectively expands the footprint of these features in time-1 so they

can be compared accurately to the time-2 image, even if slightly misregistered. As seen in Figure 5.5, this filter eliminates false detections caused by misalignment of one or two pixels.

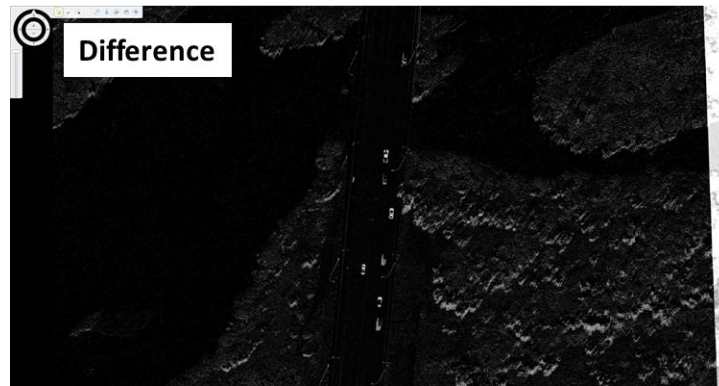


Figure 5.4. Difference images for a bridge in Albuquerque, NM. Changes associated with shadow movement over time are apparent in the difference image, and these changes are not of interest for post-hazard damage assessment.

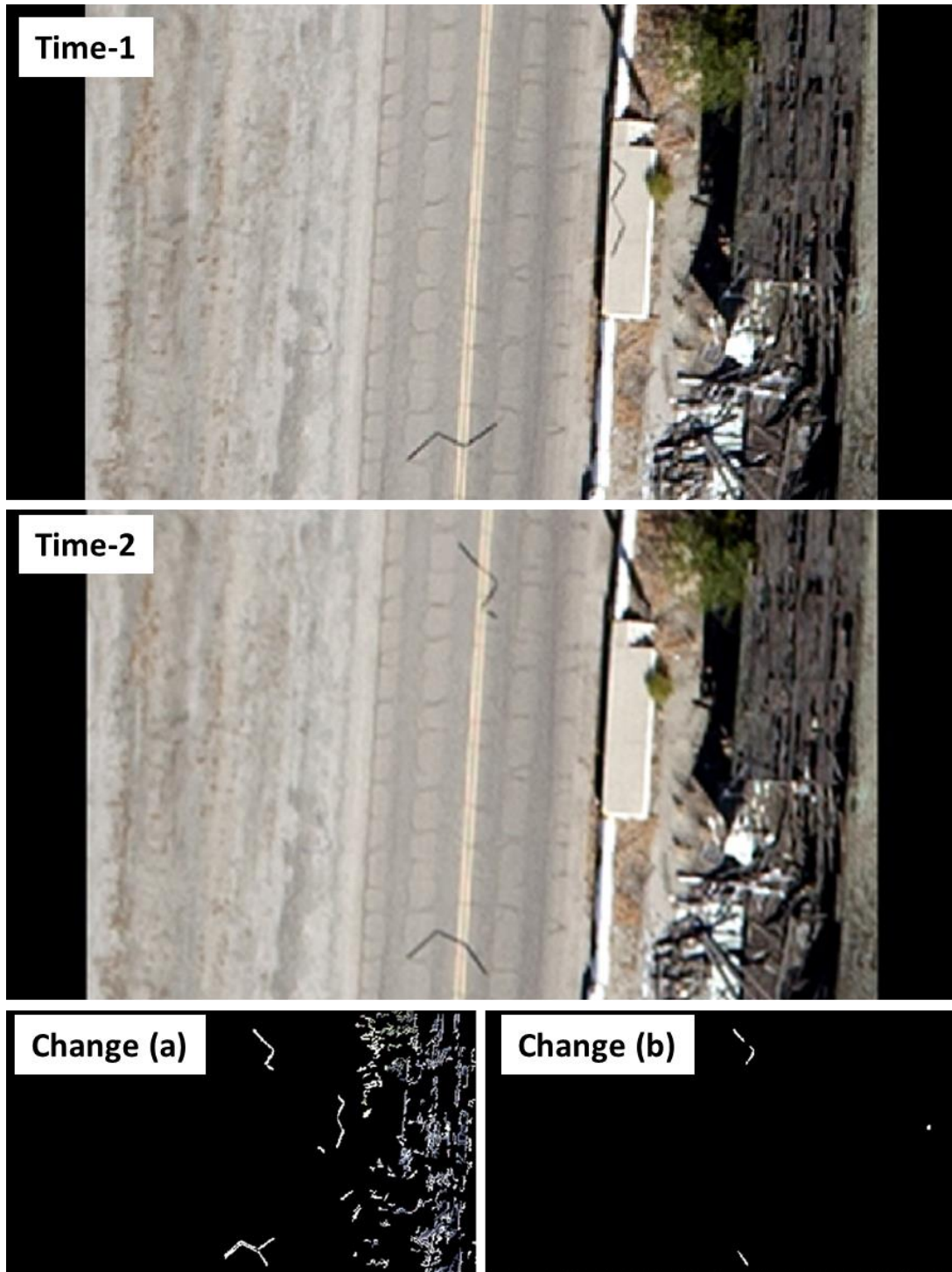


Figure 5.5. Time-1, time-2, and change images (black = no change, white = change) for an area on Camp Roberts, CA, with abandoned barracks and a marching deck. Change image (a) (bottom left) was derived with no focal filter applied to correct for misregistration, while the right-most change image (b) was derived with misregistration correction.

After masking out areas where cracks are present in the time-1 image and removing effects of misregistration, a difference image is created (by subtracting time-1 from time-2), and a threshold is applied to determine where substantive changes have occurred and classify difference values as representing change or no-change. The resulting product is a two-class image depicting either change or no change pixels. With the change detection product generated, the process moves on to a stage of classifying changes as representing crack damage or not. As new cracks are changes of interest and are manifested as elongated, narrow objects, a series of kernel based focal majority filters is used to identify changes fitting this criterion. With each pass of the majority filter over the binary change image, change features are eroded from the outside in. Narrow features such as cracks are completely eliminated by this process after only a few passes. Therefore, objects that are present in the initial threshold classified difference image, but eliminated by the series of majority filters are retained as possible cracks. This process successfully eliminates the detection of cars, a primary change feature not of interest.

The most difficult change not of interest to successfully ignore is moving shadows created by light and sign posts lining roadways. These features share many spectral and spatial characteristics of cracks. They are elongated linear regions that are manifested as a decrease in brightness from time-1 to time-2. To eliminate these areas from consideration, the results of a shadow detection algorithm may be used to mask areas that exhibit shadows only in time-2. This solution is imperfect, as there is the possibility of changes of interest being present in the same region that are shadowed in time-2 only. The solution has been effective as a result of limited shadowing present on road and bridge surfaces not caused by light and sign posts. The method would be less successful in areas with significant shadow areas caused by overhanging vegetation or buildings.

With spurious detections eliminated, the final product presented to the image analyst is a visually simple image with newly detected cracks highlighted in red. The change detection process described above is successful at identifying all new cracks, while presenting few false detections. Figure 5.6 shows change detection products generated using 1.5" (4 cm) imagery from Albuquerque, NM, after all enhancements and spatial filters were applied.

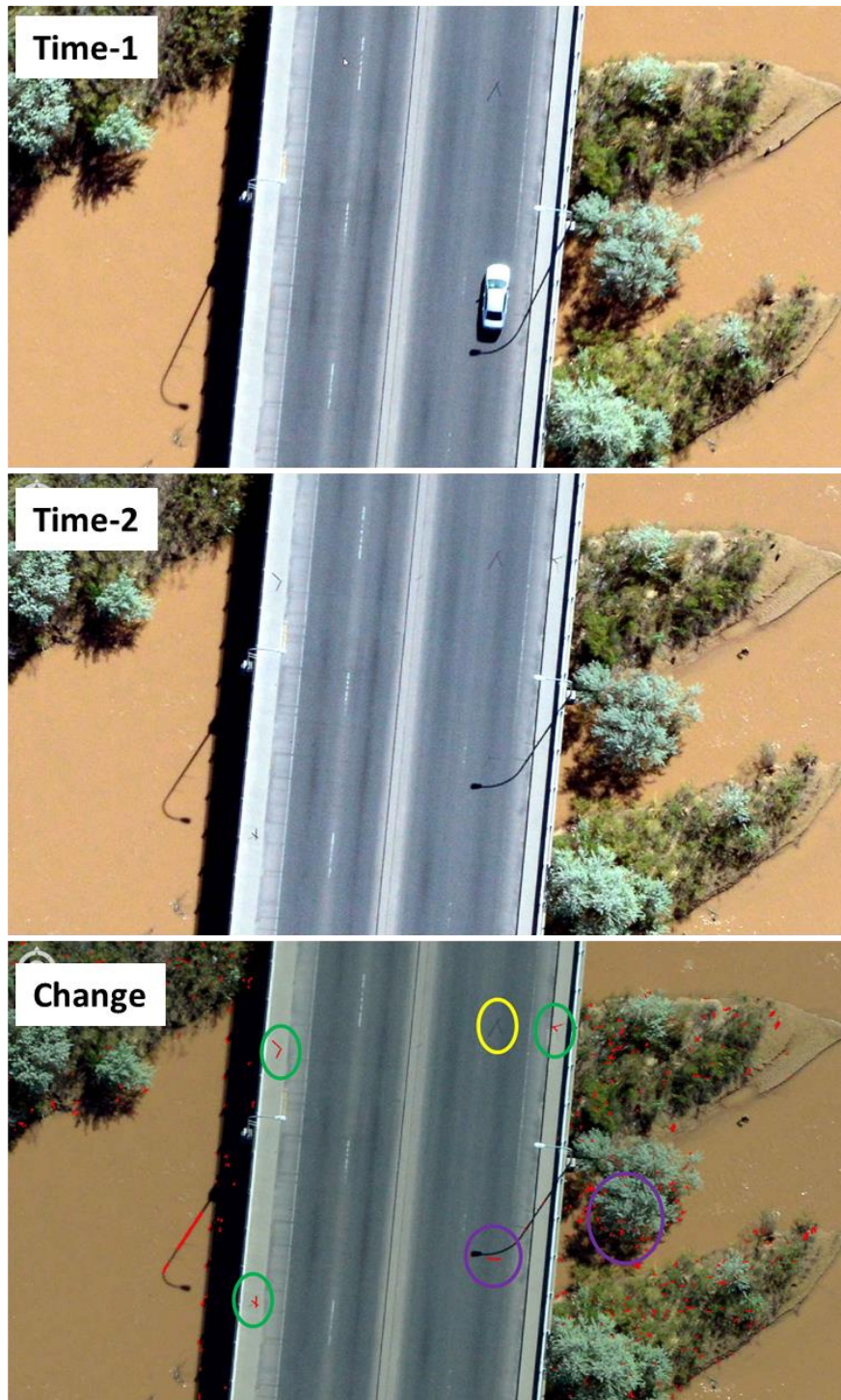


Figure 5.6. Zoomed in view of final change product. Detected changes in the “change” image (bottom), are shown in red superimposed on the time-2 image. All new simulated changes are detected (green circles), and existing simulated cracks are not detected as a change (yellow circle). False changes are limited to the shadow of a car bumper and shadow movement outside of the bridge surface (purple circle).

Shadow correction

Key sources of brightness variability between multi-temporal aerial frame images include atmospheric and illumination conditions, camera exposure settings, and shadows that change in orientation or extent. Shadows have the greatest effect on the comparison of image brightness values over time, and may lead to errors and insensitivities in change detection, image classification, and geometric co-registration (Benediktsson and Sveinsson 1997; Wang et al. 1999). Therefore, the majority of the effort related to image enhancements or adjustments supporting change detection was focused on shadow detection and normalization. Shadow changes between multitemporal image collections introduce: (1) spectral-radiometric (SR) differences that are similar or greater in magnitude than those of the changed features of interest, (2) time-varying effects on image texture, and (3) limited dynamic range in digital number (DN) values within shadow areas.

Detecting and classifying shadows is the basis for either ‘masking out’ (i.e., removing) or radiometrically normalizing (i.e., correcting) shadowed areas for change detection processing. Normalization of shadows is the process of adjusting DN values of pixels within shadows in order to approximate directly-illuminated conditions (Li et al. 2014). Traditional approaches to shadow detection and normalization are insufficient to support rapid, accurate, and reliable change detection based on multi-temporal very high (spatial) resolution (VHR) aerial frame imagery. The team developed and evaluated the utility of an approach that exploits SR differences between RSI pairs as a basis for shadow detection and normalization, in the context of detailed image change detection.

The team utilized temporal ratios of intensity and intensity-normalized blue waveband as a basis for detecting transient shadows. Figure 5.7 shows bi-temporal shadow classification maps of the four study scenes used for algorithm testing and development.

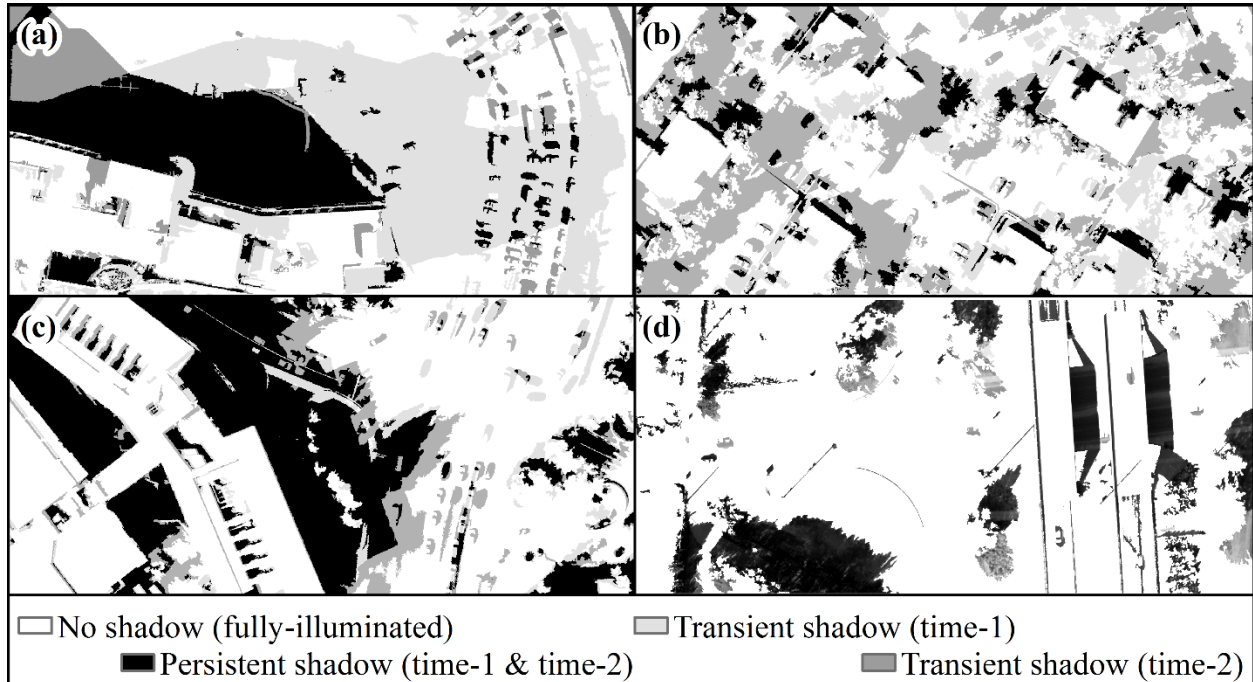


Figure 5.7. Bi-temporal shadow classification maps of the four study scenes, corresponding to (a) frames *a* and *b* (hospital facility), (b) *c* and *d* (office park), (c) *d* and *e* (university campus), and (d) *f* and *g* (bridge overpass).

The bi-temporal shadow maps provide a basis for normalizing intensity values within the transient shadow regions, using values of mean and variance per unit. The original (non-normalized) and normalized intensity image pairs of the hospital facility scene are shown in Figure 5.8, along with arithmetical difference images based on the original and normalized intensity image pairs. The brightness variation resulting from shadows in the original images leads to the false appearance of change in the difference image, which reduces detectability of actual physical changes in the scene. In contrast, the difference image derived from shadow normalized images does not exhibit high magnitude differences where shadows are different between time-1 and time-2, and would enhance assessments of physical changes of interest in the scene. Finer-scale results of shadow normalization are illustrated in Figure 5.9.

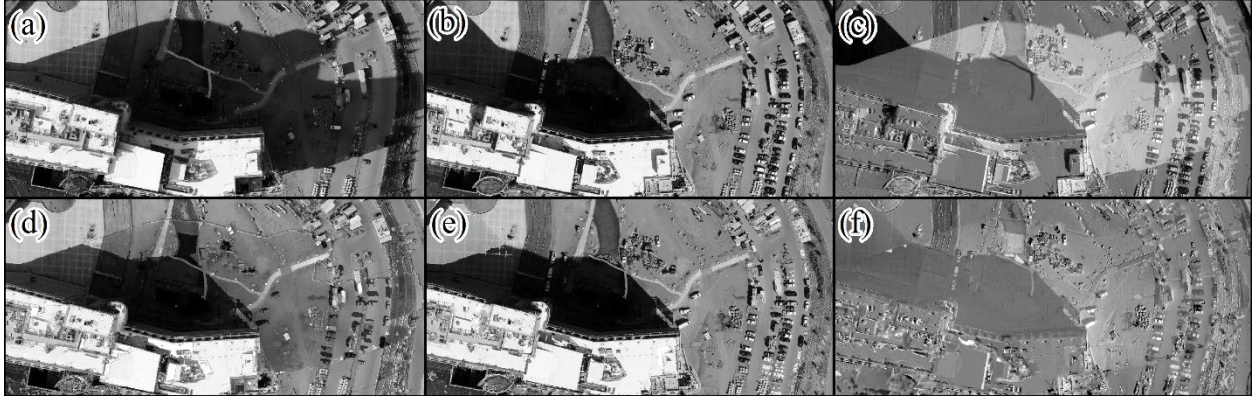


Figure 5.8. Comparison of intensity image difference products based on the normalized images versus the original intensity images. The original intensity images at (a) *time-1* and (b) *time-2* were subtracted to generate (c) a difference image, wherein neutral (no or little change) is grey while black and white shades represent high negative and positive intensity changes, respectively. The frames labeled (d) and (e) represent the *time-1* and *time-2* intensity images which were normalized in transient shadow areas, and frame (f) shows their arithmetical difference.

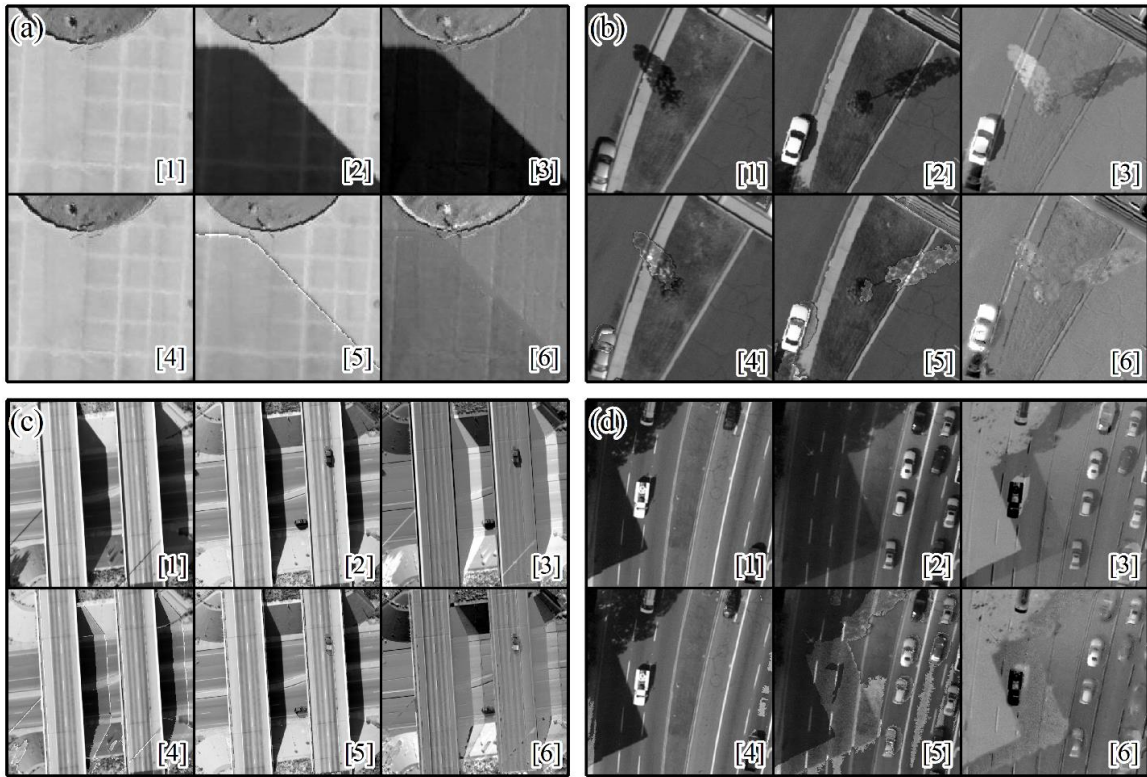


Figure 5.9. Magnified subsets of the intensity and arithmetical difference products, based on normalized images *versus* original images. The subsets are located within the (a) hospital facility, (b) office park, (c) bridge overpass, and (d) university campus scenes. Subset images are co-organized as: [1] original intensity image at *time-1* and [2] *time-2* used to generate [3] an arithmetical difference image; subsets [4] and [5] represent the *time-1* and *time-2* intensity images which were normalized in transient shadows, and [6] arithmetical difference. Neutral (no or little change) is grey while black and white shades represent negative and positive changes, respectively.

It is evident from Figures 5.8 and 5.9 that the shadow-normalized products greatly reduce the magnitude and extent of SR artifacts in bi-temporal difference images which are associated with transient shadows. Figure 5.8(a) shows a cement surface in transient shadow which was normalized to approximate directly-illuminated conditions with a high degree of fidelity artifacts. Commission error in the transient shadow classification are evident through the shadow normalization in Figure 5.9(b), where some rays of light penetrating a tree canopy were misclassified as shadow and brightened. Nonetheless, this normalized difference image contains fewer visual artifacts related to shadow than that based on the original intensity images. In general, few errors of commission or omission in the shadow maps resulted in artifacts in the normalized intensity images. Misclassification of changed features as shadows was not prevalent.

High shadow classification accuracy is critical for the purpose of shadow masking and/or normalization (Li et al. 2014), and subsequently for change detection. Using the developed shadow detection approach that exploited multitemporal image pairs, the team obtained shadow detection accuracy values between 87-97%. Further, this work demonstrated that accurate, bi-temporal shadow maps provide a basis for normalizing transient shadows. More detailed information about the shadow detection and normalization routines described here may be found in Storey et al. (2016).

The team implemented simple shadow normalization by overlaying co-registered RSI image pairs and equalizing the intensity value distributions in transient shadow areas (based upon mean and standard deviation values). Image differencing based on the normalized products showed that this approach has potential to improve change detection accuracy by reducing the SR variations resulting from transient shadows. More advanced techniques of shadow normalization, including object-based image analysis and processing in the true-color domain, are beyond the scope of this study yet would be feasible based the general approach of overlaying time-1 and time-2 images. Overlay of the RSI pairs proved viable for shadow detection and normalization as an integrated procedure.

Chapter 6: Software Implementation

Co-registration, change detection, and image enhancement procedures were all implemented in BAE's SOCET GXP software platform. All developments described in this section were added to the standard commercial offering of SOCET GXP in order to make the developments of this project available commercially by project completion. In some cases, what was implemented in SOCET GXP represents only a partial implementation of the algorithm developments described above due to the logistics of implementing the sometimes complex algorithmic approaches derived through the project into a market ready product in the time allowed.

The software architecture can be seen in Figure 6.1. The system employs several discrete software packages offered by BAE Systems, including: (1) the desktop application SOCET GXP for bulk processing by a single trained analyst, (2) GXP WebView for remote inspection by engineers, (3) GXP Explorer for cataloguing, and (4) GXP OnScene for accessing and supplementing results based on field inspections.

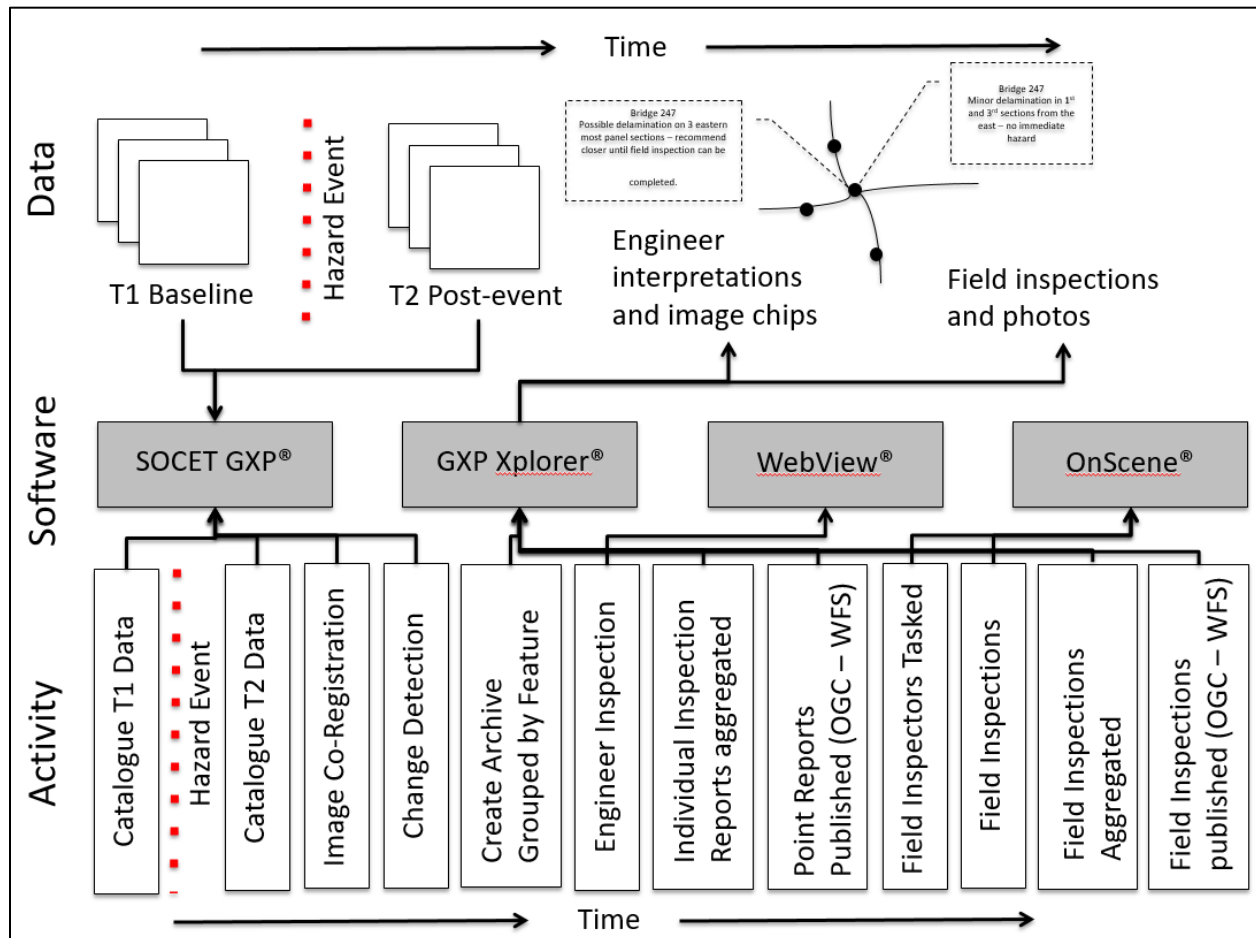


Figure 6.1: Overview figure showing how the software tools relate to the project workflow.

All processing of imagery, including co-registration, image normalization, change detection, and change enhancement is conducted within the desktop software SOCET GXP. This allows the use of a single license and a single trained analyst to operate the system. GXP Explorer, a server based platform, catalogues all image products and serves as a central repository for all products, expert interpretations, and associated metadata. WebView serves imagery and derived products to remote engineers for inspection and allows them to comment on and annotate those image products, which when submitted are stored by GXP Explorer. OnScene permits remote access to both derived image products and annotations by remote engineers while in the field and for field reports to be submitted back to GXP Explorer for central storage and access.

Automated image co-registration, as described above, was implemented into a batch process within SOCET GXP desktop software. The change detection process developed through the project could not be feasibly implemented into SOCET GXP by project termination, so a range of simpler change detection algorithms were evaluated and compared, including simple difference, relative difference, spectral angle, multi-color difference etc. The advanced pixel comparison and analysis described in (Sasagawa *et al.* 2008) was selected to derive a change image showing only the changes between two images. A multicolored change enhancement image was also implemented to aid in remote inspection. In this enhancement, unchanged pixels are displayed as gray and changes as red and cyan. This is done by displaying the intensities of the time-1 and time-2 images in red and green/blue respectively. Figure 6.2 shows the four products that are presented to remote engineers for inspection: a time-2 image, registered time-1 image, multicolored change image, and change image.

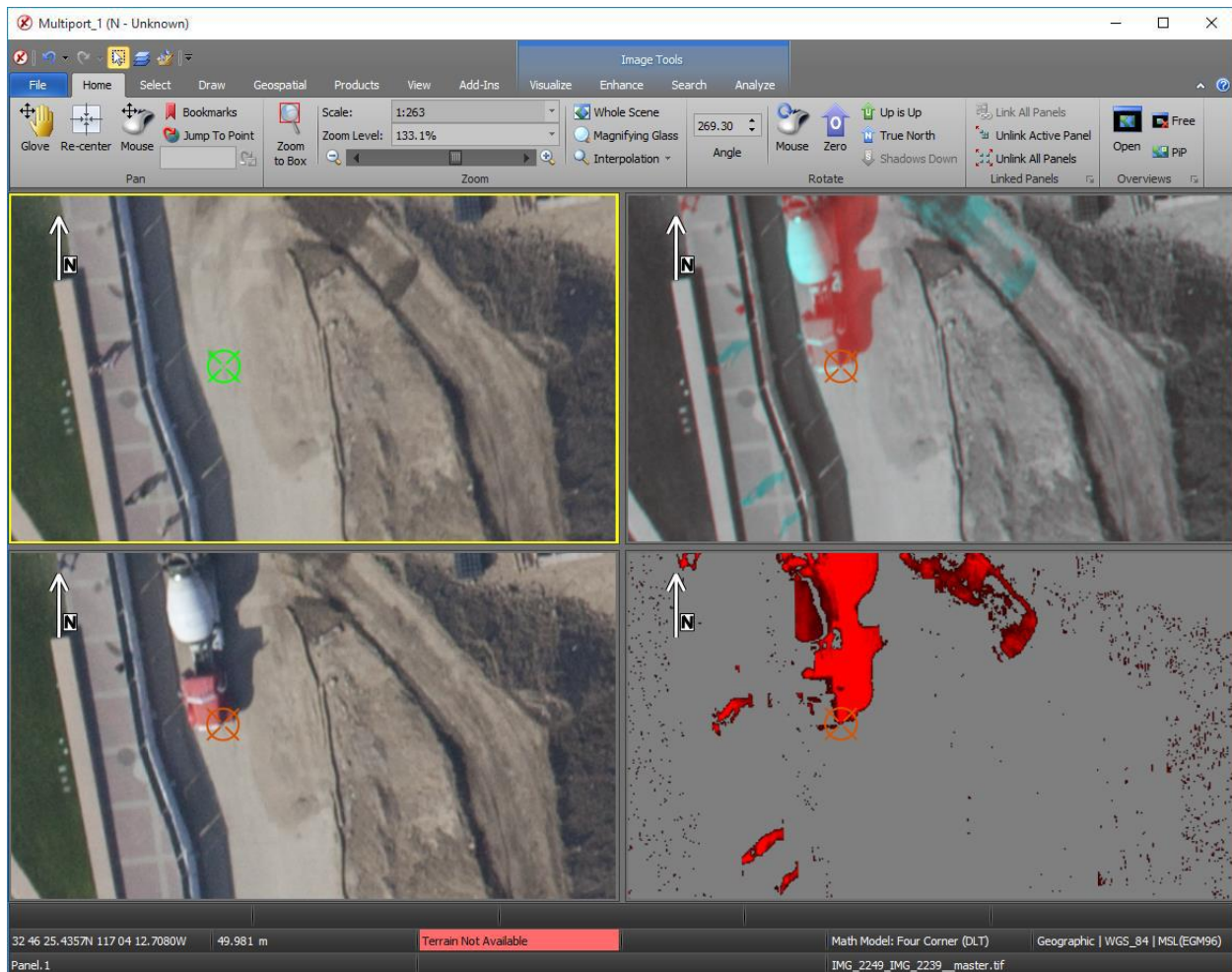


Figure 6.2. SOCET GXP showing time-2 image (top left), time-1 image (bottom left), multicolored change enhancement image (top right) and change detection result (bottom right) showing changes between the time-1 and time-2 images.

Having implemented co-registration, change detection, and change enhancement procedures into the RSI-automated change detection (RSI-ACD) batch process, attention was turned to the user experience. Specifically, the team sought to develop an optimized user interface facilitating rapid and user-friendly visualization of pre-hazard and post-hazard RSI image sets (and derived image enhancements/change products) to support post-hazard assessment of critical transportation infrastructure by DOT.

The existing user interfaces in the GXP Platform software (GXP Xplorer[®], SOCET GXP, GXP WebView, and GXP Xplorer Mobile) facilitate rapid and user-friendly visualization of RSI- ACD images created by the GXP RSI-ACD batch process. After the RSI-ACD process is completed, there are four GeoTIFF images for each image station (Time-1 baseline image, time-2 image acquired after the event, multi-colored change image; and change detection image). After cataloging in GXP Explorer, and automated process triggered by the SOCET GXP analyst, these images are

accessible from any computer anywhere that has a successful connection with the GXP Xplorer server.

After image cataloging is finished, the images can be retrieved in GXP Xplorer Map view or List view. In Map view, the user can zoom in and search all the images in a region by specifying the image type/time/defined area in the “Search By” panel. To find all the RSI- ACD images for one image station, the user can type in part of the station name or select the icons in the Map view. The resulting images are seen in the Product Gallery window (Figure 6.3).

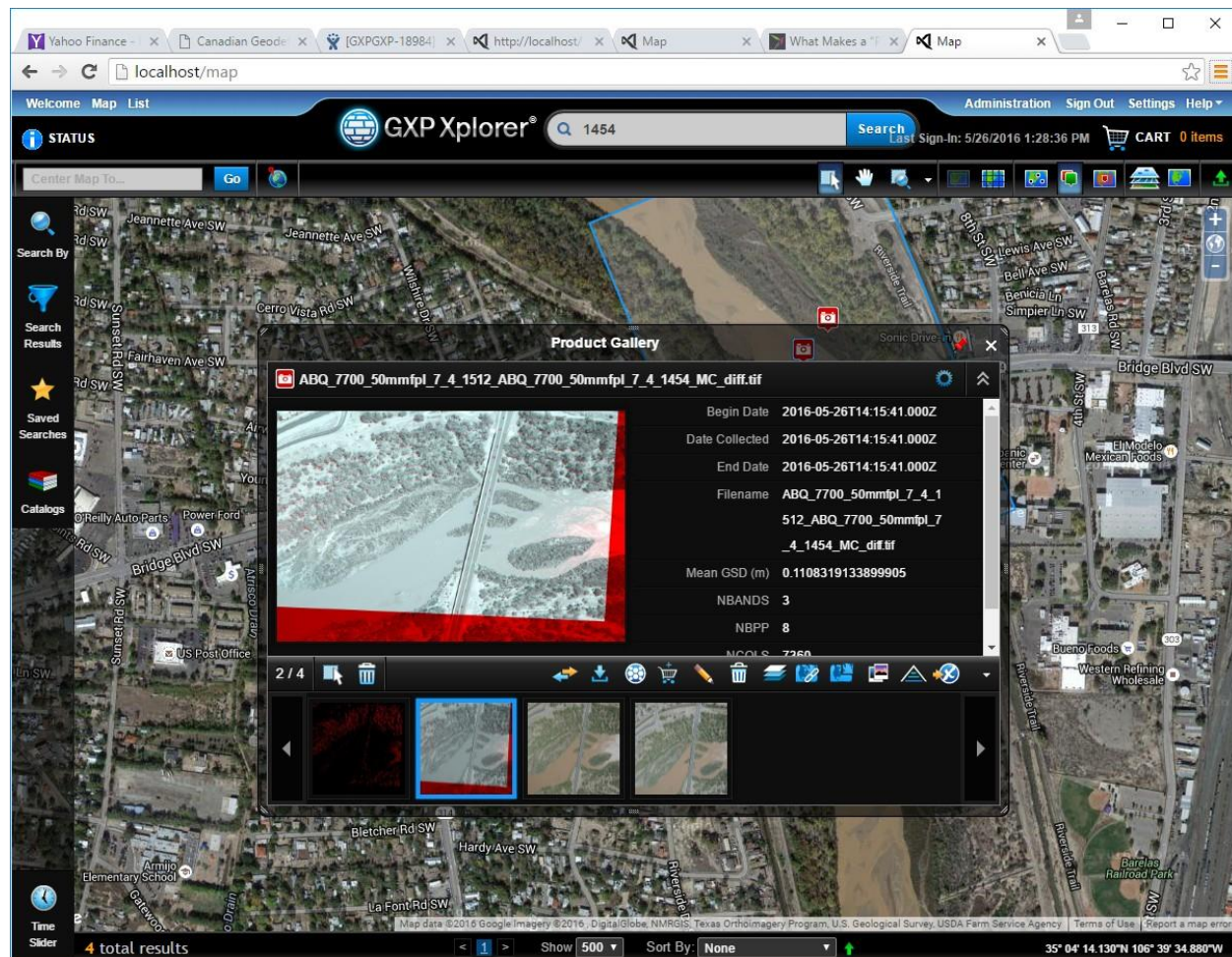


Figure 6.3. Finding images for an Image Station in GXP Xplorer.

The selected RSI-ACD co-registered images and change results can be opened in GXP WebView in the same web browser as GXP Explorer. In the GXP WebView Layer Manager, the user can turn on/off each image layer at will and assign an image to the active panel. The newly developed multi-panel feature in GXP WebView allows the user to see the four images side by side as well as in SOCET GXP desktop. The remote engineer can create markers and notes, measure the change features detected, and publish the findings in PowerPoint and JPEG formats (Figure 6.4). The user also has the option to share the image and annotations with others by uploading a JPEG image to the GXP Explorer server or sending an email with attachment.

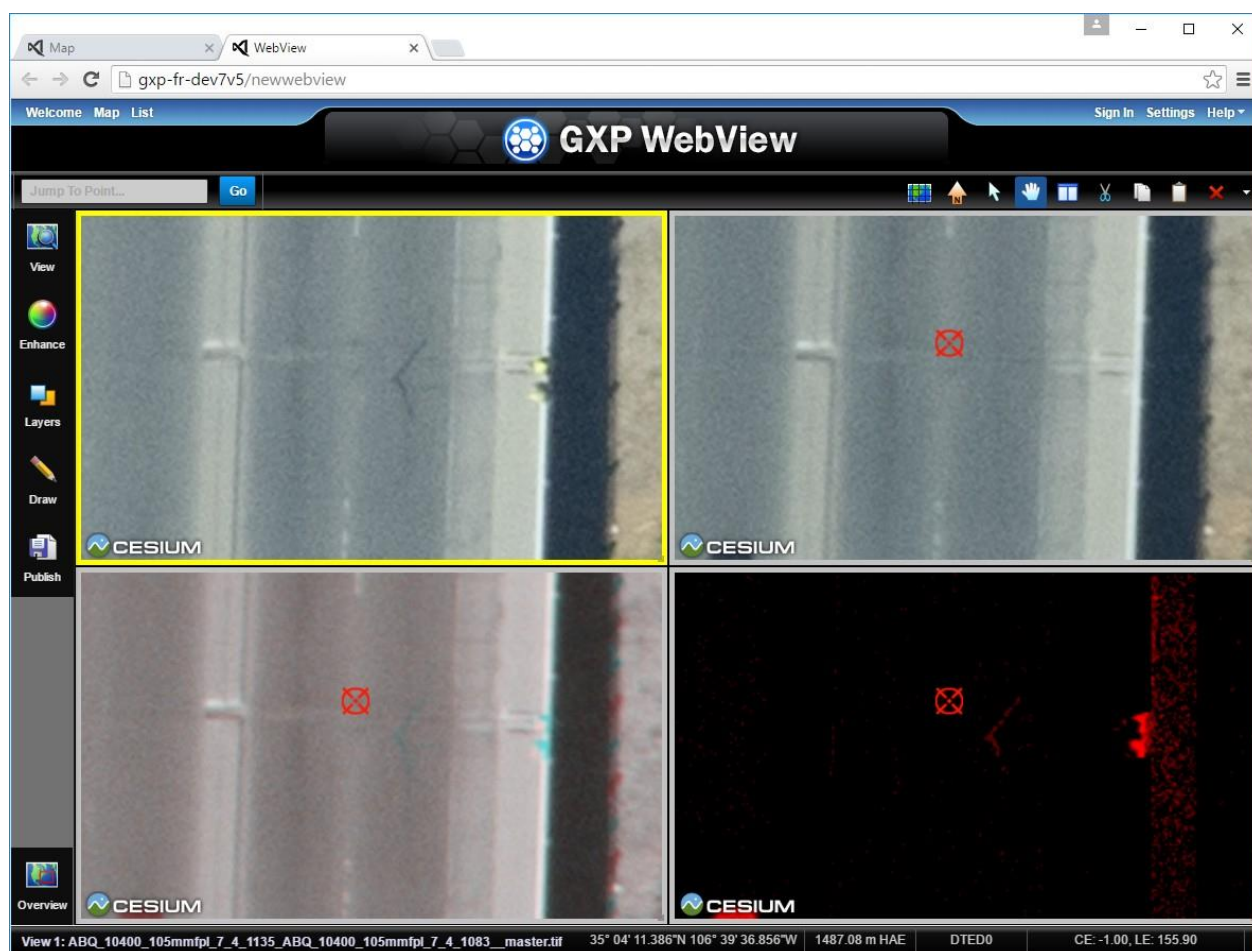


Figure 6.4. GXP WebView with multiple image layers.

The GXP OnScene Mobile app can be used to search the GXP Explorer catalog server to find and display the RSI-ACD images and already contributed results for a user-defined area on tablets, and it is possible to download an image chip (Figure 6.5). The user can also take a photo using the camera of the tablet and contribute text to create a field report and then upload it with notes to the GXP Explorer server for sharing.

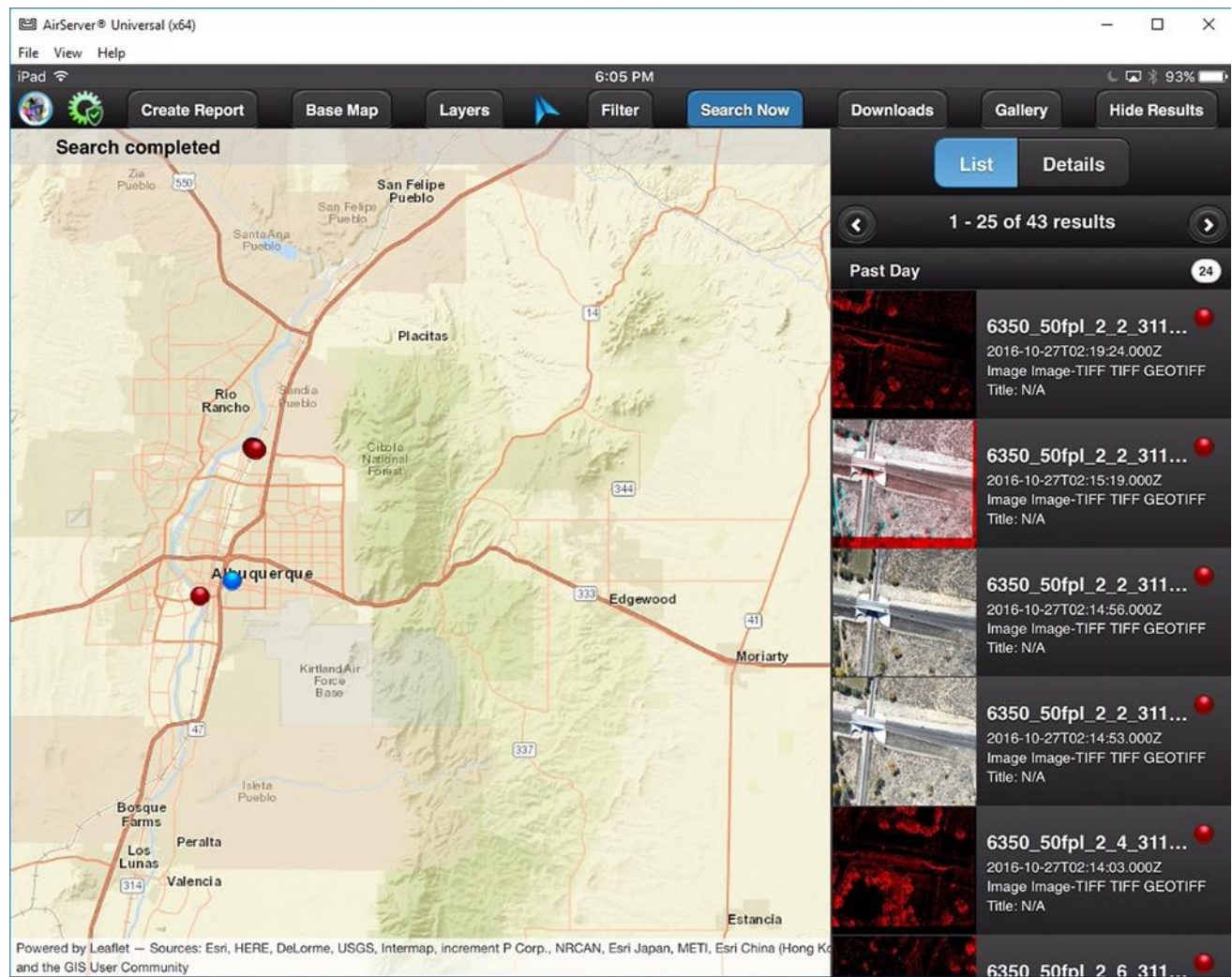


Figure 6.5: Selecting an image in GXP Xplorer Mobile.

The newly developed DAC capability allows the administrator of the GXP Xplorer server to restrict certain users to access the images only in a defined region or data source. This would enable, for example, a field crew to discover images only in its area of responsibility and not be distracted by other images across a wide area.

Chapter 7: Post-prototype Survey

Once the prototype system was developed and implemented in the GXP Platform, a second survey of NMDOT engineers was conducted. A total of 31 interviewees were identified from NMDOT's various districts, bureaus, offices, and divisions. Survey responses were obtained from 17 (55% response rate). The survey was developed to determine the qualitative utility and desirability of the products derived from an optimized TSRSS for the detection of fine scale damage to transportation infrastructure. For the surveys, the assumption was that a large-scale hazard event (earthquake) occurred in central New Mexico where transportation infrastructure assets (e.g., bridges and roads) could be damaged. Aerial images would be acquired and processed for this area within 6 hours after the earthquake and RSI products generated for condition assessment.

Interviewees were presented the after image, before and after image, enhancement image, and change detection images, and an image with multiple windows to show before, after, enhancement, and change detection images to the interviewees for utility survey, and asked: (1) how comfortable would you be making decisions to keep the bridge open for emergency personnel and evacuation? And, (2) How comfortable would you be making decisions to keep the bridge open for emergency personnel and evacuation? The interviewees answered the questions on a scale of 1 to 10 with 1 being "not comfortable at all" and 10 being "completely comfortable." Survey results reveal that transportation managers think after images, before and after images, enhancement images, change detection images, and multiple window images can be used to assist their decision making regarding keeping the bridge/road open or not. The median values of decision comfortability for bridges range from 2 to 4 while the median values of decision comfortability of roads range from 6 to 7. Results also reveal that most (>75%) transportation infrastructure managers feel more comfortable to make decisions for roads rather than bridges.

Transportation managers were also asked to rate the overall usefulness of the optimized TSRSS products in terms of assisting their decision-making following a large hazard event and in terms of assisting their decision-making in routine assessment. They were asked to rate the level of usefulness as an index on a 4-point scale, with 1 being "not useful," 2 being "neutral or unsure," 3 being "useful," and 4 being "very useful." The median value of overall usefulness for post-disaster condition assessment and routine condition assessment are 3 and 3 respectively. This indicates that transportation managers think the optimized TSRSS is useful for both post-disaster condition assessment and routine condition assessment. However, the usefulness for post-disaster condition assessment ranges from 2 to 4, while the usefulness for routine condition assessment ranges from 1 to 4. This indicates that transportation infrastructure managers feel more comfortable to use the optimized TSRSS for post-disaster condition assessment.

As mentioned previously, the assumption is that the optimized TSRSS products (i.e., before and after images, enhancement images, and change detection images) can be presented to the transportation managers within 6 hours from the hazard event based on modeling with ADAPTTE. To understand how the timeliness of the optimized TSRSS products affects manager's decision making, transportation managers were also asked if producing these products within 3

hours would improve their ability to manage assets, and if producing these products within 9, 12 or 24 hours would decrease their ability to manage their assets. 13 out 16 (82%) of the interviewees indicated that shorter than 6 hours would improve their response ability, while longer than 6 hours would decrease it.

In summary, the transportation managers interviewed indicate that there is substantial promise in implementing the designed and commercialized capabilities. They also indicate that steps to further expedite information delivery and to implement the developed capabilities for oblique imagery are warranted to improve the systems utility, particularly for bridge inspections. Modeling in ADAPTTE indicates that UAS holds great potential to improve the timeliness of delivery, and UAS routinely equipped with gimbal mounts makes them suitable for oblique imaging. The technical and administrative challenges involved in large scale rapid deployment of UAS over United States cities, however, make manned airborne the only practical solution in the immediate term.

Chapter 8: Commercialization Plan

The research and development project that this report summarizes was conducted in cooperation with BAE Systems Inc. All software developed through the project has been implemented within BAE's GXP platform, which is already used widely throughout the United States government, particularly within the defense and intelligence arena. Therefore, all software and analytical workflows developed through the project are now commercially available for purchase through an established, supported product. Furthermore, BAE currently holds an indefinite duration indefinite quantity (IDIQ) contract with the US Department of Homeland Security for imaging immediately following federally declared disaster events, including operating a network of aircraft and sensors staged for rapid deployment. The current commercial status of the developed products is therefore obtainable as a software product for internal program development, as service conducted by BAE Systems Inc., or as a service conducted by a third party company or agency.

During and after the final demonstration in Albuquerque, NM, attention was turned to the commercialization of the development. The first step was to approach the New Mexico DOT (NMDOT) engineers who attended the event, but this was not fruitful. This immediately suggests an important inference: the system may be too complex for use by non-experts, but it would probably be valuable if provided in the form of a service. This informal inference is supported by the survey of NMDOT, from which finding suggest that NMDOT does not currently have the infrastructure to support the deployment of the designed system.

A series of teleconferences have been convened by Dr. Lippitt consisting of a subset of the stakeholders, i.e. representatives of UNM, BAE Systems and SDSU, together with TAC member Dr. Bruce Davis, who is intimately aware of federal disaster response procedures and agencies. These teleconferences will continue monthly or bimonthly through 2017. In parallel, UNM will take the lead in maintaining contact with OST-R so that the group can respond in a timely fashion to new initiatives and opportunities at OST, for example in FHWA.

At the teleconference on 9 December 2016, for example, the discussion was focused on transportation, but it was acknowledged that there are multiple applications of automatic change detection and that other agencies, e.g. DHS, DoD (NGA) and FEMA, may have an interest.

Graduate students at UNM have applied for Innovation Corps (I-Corps™), a program to leverage federal investments in research and help them across the commercialization "Ditch of Death." This was described by Santiago Navarro of OST-R at the workshop in Oklahoma City on 2 December 2015. A possible route would be submission of an unsolicited white paper. Such an approach may also be appropriate for DHS. It was agreed that the creation of a white paper, which could be modified and used as appropriate in submissions for funding, is one essential to commercialization, so this will be a priority after the formal closure of the project. Previous work by SDSU on their WATSCIN algorithm for multi-temporal change detection led to a white paper addressed to DHS, which could perhaps be used as a model. In particular, several State DOTs, for example New York DOT, are open to receiving unsolicited white papers and have limited R&D

funds to disburse, so these must be approached. Many others, however, have formal procedures for R&D, such as SBIR/STTR, which are more onerous in terms of the group's resources, so the team has to identify and pursue the most promising avenues. Clearly, there is no problem complying with the requirement to involve a research institution and it would also be possible to comply with small business requirements using small businesses with which the partners are familiar. The effort is almost entirely US-based, but the group will also look at practices in countries such as Denmark and Sweden, where airborne monitoring of infrastructure is already routine.

BAE Systems wishes to participate in the commercialization, though it has made clear that the two SDSU algorithms described convincingly in Albuquerque – crack delineation and shadow normalization – do not have an immediate market amongst its predominantly defense-based customers, so funding would be required to integrate these into the commercial product, which would be a straightforward task from the technical point of view. A routine product development that is already being executed as part of the evolving GXP roadmap, is highly relevant. The GXP OnScene mobile app will eclipse its predecessors, GXP Xplorer Mobile and GXP Snap, and is being enhanced by the capability of including user-designed forms that can be completed in the field. Such a form, for example, could be a digital version of the form that NMDOT currently uses in the field to assess damage, with completion by means of a pen or pencil.

A high priority, in addition to the creation and transmission of unsolicited white papers, is more general marketing. Conference presentations, given or planned, at events related to military ISR, homeland security, transportation, photogrammetry/remote sensing/GIS and emergency management represent the team's primary approach. This effort can be increased if it seems promising. Many of the application areas, of course, are broader than detecting changes to highway infrastructure, but all of them require automatic change detection and benefit considerably from the implemented and automated RSI approach. In many cases, presentations and networking efforts at national conferences could pay dividends, but some organizations, such as FEMA, have regional structures, so the team needs to determine how best to work at this disaggregated level.

Since the solution is based on commercial software, cost is a source of anxiety for many DOTs, so BAE Systems should investigate an attractive pricing structure, perhaps based on a consumption model, whereby users would pay for the software during training, updates, ingest of the before imagery, practice drills and emergency management, but not while the software is dormant. This is not commercially attractive *prima facie*, but could be a valuable competitive advantage in the future, for example, with a pricing model designed specifically for emergency management applications. Furthermore, it is likely that the functionality of the heavy SOCET GXP desktop application will be transferred through time to the browser-based GXP WebView. For example, the whole system would then be server-based and hosted in a public or private cloud, which would facilitate the implementation of novel pricing models.

The team is aware that some public agencies prefer not to invest in mapping software, but contract to commercial mapping companies. In this case, the team must find a solution amenable

to all parties. BAE Systems itself has a history of offering services in the area of geospatial data generation and currently has an IDIQ with DHS to respond, via a network of commercial companies with capabilities for rapid acquisition of aerial photography, with up-to-date geospatial data of disaster areas in less than 48 hours. A variant of this using CAP could doubtless be developed for transportation. It is likely that BAE could leverage contacts in DHS, such as Dr. David Alexander or appropriate DHS managers involved with the BAE Systems contract, to better understand the customer expectation in terms of data quality, user experience, timeliness of response, pricing, etc. For example, it would be necessary to establish, together with CAP, standards for keeping the before imagery up to date and for flying the after imagery in conditions that could be extremely demanding, such as excessive wind and/or turbulence after hurricanes or tornadoes. It may be possible to explore a contract modification to the existing DHS IDIQ to add RSI capabilities. There would be no need to change the processing arrangements or the software, since the BAE Systems business area involved already uses GXP software, but the current IDIQ uses private survey companies so it is not clear how to involve CAP in a way that is contractually and politically acceptable. GXP has contacted colleagues involved in the DHS IDIQ as a first step.

The team is also pursuing business development with Customs and Border Patrol (CBP), which is an existing customer of both SDSU and BAE Systems. Mr. Coulter of SDSU met with CBP at the Pentagon on 15 December 2016 and a follow-up meeting is planned for February 2017 at SDSU. The focus is implementation of SDSU's WATSCIN algorithm for *multi-temporal* change detection – people and vehicles in border areas – but RSI would bring clear advantages. A new application that has not been investigated yet is for the FAA – finding change at or around airports. The team is familiar with the obstruction surfaces that have to be created and monitored around airports, but rapid change detection between formal, expensive surveys could be a very useful, additional input.

The discussion above has a wide compass and extends into application areas beyond the DOT. Highway infrastructure is the primary goal of the commercialization effort, however, and one of the ongoing initiatives is a systematic investigation of all the DOT funding vehicles for R&D at both federal and state levels. BAE Systems has already begun work on this study. A starting point was the presentation on funding sources by Dr. Sreenivas Alampalli, New York State DOT, at the workshop in Oklahoma City on 2 December 2015. Dr. Alampalli gracefully accepted a visit by Dr. Stewart Walker of BAE Systems on 8 November 2016 to discuss this topic further and the resulting notes are providing directions for the investigation.

All tools developed through this research and development project are now commercially available, either as a software product for purchase or as a service from BAE Systems Inc. or a third party. Commercialization efforts, mainly in the form of customer development, are ongoing. The inclusion of an established commercial partner and embedding of tools into an existing and supported software package have enabled a product at TRL 9 within the span of a 2-year project.

Chapter 9: Conclusions

This research project aimed to develop a remote sensing system capable of rapidly identifying fine-scale damage to critical transportation infrastructure following hazard events. Such a system must be pre-planned for rapid deployment, automate processing routines to expedite the delivery of information, fit within existing standard operating procedures to facilitate ready use during a hazard response scenario, and the tools need to be commercially available to DOTs. To design the system and meet these needs, the project team designed an airborne remote sensing system based on a network of collection platforms, an automated image co-registration and change detection routine, and implemented all software tools within BAE Systems' GXP line of geospatial software. A version of all image-processing and interpretation tools developed through the project are now commercially available from BAE Systems Inc. and the project team is actively working to implement the programs with state DOTs and federal agencies.

References

- Ambrosia, V.G., S.S. Wegener, D.V. Sullivan, S.W. Buechel, S.E. Dunagan, J.A. Brass, J. Stoneburner, S.M. Schoenung
2003 Demonstrating UAV-acquired real-time thermal data over fires. *Photogrammetric Engineering & Remote Sensing*, 69(4): 391-402.
- BAE Systems, 2017. SOCET GXP®v4.2.0: Advanced geospatial exploitation and customized product creation combined into one comprehensive solution.
<http://www.geospatalexploitationproducts.com/content/socet-gxp/>, last viewed 6 January 2017.
- Benediktsson, J. A., and J.R. Sveinsson.
1997 Feature extraction for multisource data classification with artificial neural networks. *International Journal of Remote Sensing*, 18(4), 727–740.
- Bernard, Sklar
2001 *Digital communications: fundamentals and applications*. Prentice Hall, Englewood Cliffs, NJ.
- Bernsdorf, S., R. Barsch, M. Beyreuther, K. Zaksek, M. Hort and J. Wassermann
2010 Decision support system for the mobile volcano fast response system. *International Journal of Digital Earth*, 3, 280-291.
- Bradski, G. and A.Kaehler
2008 *Learning OpenCV: Computer Vision with the OpenCV Library*. O'Reilly Media, Cambridge, MA.
- CEOS
2005 The use of earth observing satellites for hazard support: Assessments and scenarios. NOAA: Brussels, Belgium.
- Cervone, G., M. Kafatos, D. Napoletani and R. P. Singh
2006 An early warning system for coastal earthquakes. In *Natural Hazards and Oceanographic Processes from Satellite Data*, pp. 636-642. Oxford: Elsevier Science Ltd.
- Chan, J. C. W., Chan, K. P., & Yeh, A. G. O.
2001 Detecting the nature of change in an urban environment: A comparison of machine learning algorithms. *Photogrammetric Engineering and Remote Sensing*, 67(2), 213-225.
- Coulter, L. , D. Stow and S. Baer
2003 A frame center matching approach to registration of high resolution airborne frame imagery. *IEEE Transactions on Geoscience and Remote Sensing*, 41 (11): 2436-2444.

Coulter, L. and D. Stow

2005 Detailed change detection using high spatial resolution frame center matched aerial photography. In *Proceedings of the 20th Biennial Workshop on Aerial Photography, Videography and High Resolution Digital Imagery for Resource Assessment*, October 4-6, 2005, Weslaco, Texas.

Coulter, L. and D. Stow

2008 Assessment of the spatial co-registration of multitemporal imagery from large format digital cameras in the context of detailed change detection. *Sensors*, 8(4): 2161-2173.

Coulter, L., D. Stow, S. Kumar, S. Dua, B. Loveless, G. Fraley, C. Lippitt and V. Shrivastava

2012 Automated co-registration of multitemporal airborne frame images for near real-time change detection. In *Proceedings of the ASPRS Annual Conference*, March 19-23, 2012, Sacramento, CA.

Li, H., L. Zhang, and H. Shen

2014 An Adaptive Nonlocal Regularized Shadow Removal Method for Aerial Remote Sensing Images. *Geoscience and Remote Sensing, IEEE Transactions on*, 52(1), 106–120. DOI 10.1109/TGRS.2012.2236562.

Otsu, N.

1975 A threshold selection method from gray-level histograms. *Automatica*, 11(285-296), 23–27.

Sasagawa, A., K. Watanabe, S. Nakajima, K. Koido, H. Ohno and H. Fujimura

2008 Automatic change detection based on pixel-change and DSM-change. *The International Archives of the Photogrammetry, Remote Sensing and Spatial Information Sciences*, XXXVII (B7): 1645-1650. Beijing, China. http://www.isprs.org/proceedings/XXXVII/congress/7_pdf/10_ThS-18/20.pdf. Last visited 6 January 2017.

Song, C., Woodcock, C. E., Seto, K. C., Lenney, M. P., & Macomber, S. A.

2001 Classification and change detection using Landsat TM data: When and how to correct atmospheric effects? *Remote Sensing of Environment*, 75(2), 230-244.

Storey, E., D. Stow, L. Coulter, and C. Chen.

In press. Efficient detection of shadows in aerial repeat station image pairs to support shadow normalization and change detection. *GIScience and Remote Sensing*.

Stow, D., L. Coulter and S. Baer

2003 A frame centre matching approach to registration for change detection with fine spatial resolution multi-temporal imagery. *International Journal of Remote Sensing*, 24(19): 3873-3879.

Stow, D., L. Coulter, G. MacDonald, and C. Lippitt

2015 Evaluation Of Geometric Capture And Processing Elements. In *The Context Of A Repeat Station Imaging Approach To Registration And Change Detection*. Report delivered to United States Department of Transportation (USDOT) Office of the Assistant Secretary for Research and

Technology (OST-R) Commercial Remote Sensing and Spatial Information Technologies Program (CRS&SI), cooperative agreement # OASRTRS-14-H-UNM.

Stow, D., L. Coulter, C. Lippitt, G. MacDonald, R. McCreight and N. Zamora
2016a Evaluation of geometric elements of Repeat Station Imaging and registration.
Photogrammetric Engineering and Remote Sensing, 82 (10): 775-788. Doi:
10.14358/PERS.82.10.775

Stow, D., H. Lan, A.S. Walker, C. Lippitt, L. Coulter, E. Storey, C. Chen, E. Schweizer, and S. Shang
2016b Automated Change Detection with Airborne Imagery for Rapid Post-hazard Transportation Assessment. Report delivered to United States Department of Transportation (USDOT) Office of the Assistant Secretary for Research and Technology (OST-R) Commercial Remote Sensing and Spatial Information Technologies Program (CRS&SI), cooperative agreement # OASRTRS-14-H-UNM.

Toutin, T.
2004 Review article: Geometric Processing of Remote Sensing Images: Models, Algorithms and Methods. *International Journal of Remote Sensing*, 25(10), 31. Doi: 1366-5901

Wang, B., A. Ono, K. Muramatsu, and K. Fujiwara
1999 Automated detection and removal of clouds and their shadows from Landsat TM images.
IEICE Transactions on Information and Systems, 82 (2), 453–460.

Appendices

Available for download on University of New Mexico GIScience for Environmental Management (GEM Lab) webpage: <http://gem.unm.edu/index.php/funded-projects/10-remote-sensing-of-transportation-infrastructure>

Appendix A: Summary of Tasks

Summarizes all tasks completed as part of project. Individual deliverables and the date each was submitted are outlined in Table A. These deliverables include meetings, reports, submission of publications, and activities such as data collection and demonstrations.

Appendix B: TAC Meeting Minutes

The meeting minutes from all four Technical Advisory Council (TAC) meetings are presented. These meetings were held on: April 8, 2015; September 25, 2015; April 4, 2016; and October 21, 2016.

Appendix C: Media, Publications, and Presentations

A list of popular media coverage, peer-reviewed publications, and academic presentations related to results generated through the project.